Chapter 2
Introduction to Quantum Many-Body Physics

In the introduction to his 1929 paper on many-electron systems [1], Dirac envisioned that the two problems facing quantum mechanics were "in connection with the exact fitting in of the theory with relativity ideas" on the one hand, and the fact that "the exact application of these laws leads to equations much too complicated to be soluble" on the other. These two problems would dominate theoretical physics throughout the twentieth century: Whereas the former led to the formulation of relativistic quantum field theories and, ultimately, the standard model of particle physics, the latter posed the central problem for the field of quantum many-body physics.

In a way that Dirac could not foresee, the quantum many-body problem continues to puzzle physicists. Although a set of theoretical and computational methods has been developed to solve most problems in atomic and nuclear physics, there is still a class of problems that defy any satisfactory solution. These are the problems for which the quantumness of the physical world is most pressing, making any treatment with classical concepts and computers intractable. For the same reasons, these are the most interesting problems for a physicist wanting to explore new physical phenomena.

In 1935 Schrödinger already noted that *entanglement* is the "characteristic trait of quantum mechanics, the one that enforces its entire departure from classical lines of thought" [2], a trait that was problematized by Einstein in the same year [3]. Yet, it is only in the last decades that entanglement in quantum many-body systems has been considered as the defining feature of so-called quantum phases of matter. This has led to an explosion of new insights into the quantum properties of systems with many degrees of freedom, where quantum correlations are no longer seen as a difficulty for simulating the system, but rather explored as a resource for exotic physical phenomena.

In this introductory chapter, we will give a short overview of quantum many-body physics, with an emphasis on the different ways in which entanglement determines

L. Vanderstraeten, *Tensor Network States and Effective Particles for Low-Dimensional Quantum Spin Systems*, Springer Theses,
DOI 10.1007/978-3-319-64191-1_2

the quantum behaviour of systems with many degrees of freedom. In the three last sections, we will discuss integrability, tensor networks and effective particle descriptions in more detail, as we will need these concepts in the following chapters.

2.1 Defining the Problem

In this dissertation we investigate the low-energy properties of systems consisting of a large number of quantum-mechanical degrees of freedom that interact locally. In this section, we explain how this is modelled mathematically, we give a physical motivation and we discuss what the interesting properties are.[1]

2.1.1 The Basics

The building block of a quantum many-body system is a d-level Hilbert space with basis vectors $|s\rangle$ ($s = 1, \ldots, d$). These elementary degrees of freedom or "spins" are brought together as parts of a large physical system, for which the Hilbert space is obtained as the direct product of all the individual spins

$$\mathbb{H} = \bigotimes_{i \in \mathcal{L}} \mathbb{H}_i .$$

The direct-product structure is a direct consequence of the superposition principle and allows for entanglement between different spins. It also implies that the size of the Hilbert grows exponentially with the number of spins, a fact that makes the quantum many-body problem notoriously difficult to deal with. In physical systems the spins are typically arranged in some spatial structure or lattice $\mathcal{L}$. In this dissertation, we are alway interested in infinitely large lattices, so that only the physics of the bulk is taken into account.[2]

A wave function for a system of N spins can be written as a superposition

$$|\Psi\rangle = \sum_{s_1,\ldots,s_N} c_{s_1,\ldots,s_N} |s_1\rangle \otimes \cdots \otimes |s_N\rangle,$$

where the $c_{s_1,\ldots,s_N}$ are complex coefficients. The wave function describes a physical state of the system, for which all physical information should in the end be obtained as the expectation value of a well-chosen operator O

[1] We assume the basic postulates and formalism of quantum mechanics [4, 5] to be in place, as well as all mathematical concepts and techniques. We refer to Ref. [6] for a modern overview.

[2] We will always ignore the mathematical difficulties of defining this thermodynamic limit.

$$\langle O \rangle = \langle \Psi | O | \Psi \rangle.$$

More generally, every state of the system is described by a density matrix ρ, acting on $\mathbb{H}$, which has expectation values

$$\langle O \rangle = \mathrm{Tr}(O\rho).$$

A model is further defined by its Hamiltonian H, modelling the interactions between the spins. We will be interested in local interactions, such that the Hamiltonian can be written as a sum of operators h_i that only act non-trivially on a small patch around site i in the lattice, i.e.

$$H = \sum_{i \in \mathcal{L}} h_i.$$

The Hamiltonian is of central importance for the physical properties of the system because

- it is associated with the time-dependence of a state $|\Psi(t)\rangle$ via the Schrödinger equation
$$i \frac{\partial}{\partial t} |\Psi(t)\rangle = H |\Psi(t)\rangle,$$
- it determines the Gibbs distribution of a system at inverse temperature β as
$$\rho = \mathrm{e}^{-\beta H}.$$

In condensed-matter systems, where one typically works at very low temperatures, one is mainly interested in the sector of Hilbert space that corresponds to the lowest eigenvalues or energies of the Hamiltonian. The eigenstate with the lowest energy is called the ground state, which determines all the static properties of the system at zero temperature, whereas the next few eigenstates or excitations determine the dynamical properties of the system.

2.1.2 Elementary Models

In classical statistical mechanics a system is often not very interesting at zero temperature, but quantum-mechanically the ground state can be a complicated state with very non-trivial properties. This can be traced back to a basic property of the Hamiltonian, viz. that the different local terms do not commute. This implies that they cannot be minimized simultaneously and that the ground state is a complicated superposition of different configurations that minimize the global energy of the state. Interestingly, the local interactions don't need to be complex in order to give rise to

interesting physics; throughout this dissertation, it will become clear that surprisingly simple Hamiltonians can give rise to an extreme variety of physical behaviour.

One paradigmatic example is the Hubbard model, which describes interacting fermions on a lattice [7]. As we will see, the Hubbard model will form the basis for a lot of models that we consider in this dissertation, so it proves worthwhile to understand how it arises as an effective model for electrons in a metal [8–10]. First of all, the assumption is made that the heavy ions in the metal's crystal form a static lattice and only the electrons are taken into account as degrees of freedom. Next, we determine one-electron wave functions in an optimal way, in the sense that the interactions between the electrons are treated as much as possible on the mean-field level. These wave functions are, because of the periodic lattice, delocalized Bloch functions that describe electrons moving independently (uncorrelated) through a potential generated by the ions and the other electrons. For some metals, this mean-field description (band theory) is not accurate enough and it proves necessary to include interactions further. This can be done by first defining Wannier functions, which are one-particle wave functions centred around a lattice site, and rewriting the second-quantized Hamiltonian in this basis as

$$H = \sum_{i,j} \sum_{\alpha,a} t_{ij} c^\dagger_{\alpha i,a} c_{\alpha j,a} + \frac{1}{2} \sum_{\alpha\ldots\delta,i\ldots l} U^{\alpha\beta\gamma\delta}_{ijkl} \sum_{ab} c^\dagger_{\alpha i,a} c^\dagger_{\beta j,b} c_{\gamma k,b} c_{\delta l,a},$$

where $c_{\alpha i,a}$ annihilates an electron in a Wannier orbital of band α, centred around site i with spin a. The simplest version of the Hubbard model is obtained by further assuming that (i) the Fermi surface lies inside a single conduction band and we are interested in low enough energies such that the other bands only determine the parameters t and U, (ii) the Wannier functions are strongly localized around one lattice site, such that only hopping matrix elements t_{ij} between nearest-neighbour lattice sites $\langle ij \rangle$ are retained, and (iii) the range of the interaction matrix elements $U^{\alpha\beta\gamma\delta}_{ijkl}$ is very small, such that only intra-atomic interactions have to be taken into account. Under these assumptions, the Hubbard model reads

$$H = -t \sum_{\langle ij \rangle} c^\dagger_{i,a} c_{j,a} + U \sum_i n_{i,\uparrow} n_{i,\downarrow},$$

where we have introduced the particle number operators $n_{i,a} = c^\dagger_{i,a} c_{i,a}$ and the diagonal hopping t_{ii} has been omitted. Despite its simplicity, the Hubbard model has been studied intensively because it captures the essential physical features of general strongly-correlated quantum systems.

Another elementary model that exhibits strongly-correlated quantum behaviour is the Heisenberg model [11], introduced to explain ferro- and antiferromagnetism in solids. It describes the behaviour of a collection of spins that are placed on fixed sites in a lattice, and is defined by the Hamiltonian

$$H = J \sum_{\langle ij \rangle} \vec{S}_i \cdot \vec{S}_j,$$

where $\vec{S}_i = \left(S_i^x, S_i^y, S_i^z\right)$ are the three spin operators. The most fundamental is the spin-1/2 model, but higher spin representations are also possible. In magnetic materials the Heisenberg interaction arises via (super-) exchange processes between effective spin degrees of freedom, where e.g. an antiferromagnetic interaction ($J > 0$) is obtained because anti-aligned spins can virtually hop to the same site and lower their kinetic energy [12]. The Heisenberg model can also be derived as an effective Hamiltonian for the Hubbard model when $U/t \gg 1$ and there is one electron per site (half-filling); indeed, in that case, the charge degrees of freedom are frozen and only the spins of the electrons remain to be taken into account.

2.1.3 Statics and Dynamics

Finding the lowest-lying eigenstates of a many-body Hamiltonian is not a goal in itself, but serves rather as a means to compute the physical, low-energy properties of the system. So what are the interesting low-energy properties of a quantum-many body system?[3]

First of all, we will be interested in thermodynamic properties such as the ground state energy density e or the average magnetization m (in e.g. the z direction)[4]

$$e = \frac{1}{|\mathcal{L}|}\langle\psi_{\text{gs}}|H|\psi_{\text{gs}}\rangle, \qquad m = \frac{1}{|\mathcal{L}|}\langle\psi_{\text{gs}}|\sum_{i\in\mathcal{L}} S_i^z|\psi_{\text{gs}}\rangle.$$

Different static susceptibilities quantify the change in these observables as a result of external perturbations such as a magnetic field or a change in temperature.

Also, we will be interested in correlation functions with respect to a given operator O

$$c(i,j) = \langle\psi_{\text{gs}}|O_i^\dagger O_j|\psi_{\text{gs}}\rangle,$$

quantifying the quantum correlations that are present in the ground state. If the operator O has a zero-temperature expectation value, it is rather the connected part of the correlation function that determines the non-trivial correlations, i.e.

$$c(i,j)_{\text{con}} = \langle\psi_{\text{gs}}|O_i^\dagger O_j|\psi_{\text{gs}}\rangle - \langle\psi_{\text{gs}}|O_i^\dagger|\psi_{\text{gs}}\rangle\langle\psi_{\text{gs}}|O_j|\psi_{\text{gs}}\rangle.$$

In typical systems, these correlation functions decay exponentially in the distance between the operators; the correlation length ξ is defined in terms of this long-distance behaviour[5]

[3] The concepts in this section can be found in more detail in standard textbooks on quantum many-body systems [9, 10, 13–15].

[4] The number of lattice sites is denoted as $|\mathcal{L}|$, which, in the thermodynamic limit, is sent to infinity.

[5] We denote $\vec{n}_i$ as the lattice vector of site i.

$$c(i,j)_{\text{con}} \to \exp\left(-\frac{|\vec{n}_i - \vec{n}_j|}{\xi}\right), \qquad |\vec{n}_i - \vec{n}_j| \gg 1,$$

and can be interpreted as an effective length scale in the system. For a translation-invariant Hamiltonian in the thermodynamic limit it makes sense to look at the momentum representation of a correlation function, the so-called static structure factor

$$s(\vec{q}) = \sum_{i\in\mathcal{L}} \mathrm{e}^{-i\vec{q}\cdot\vec{n}_i} \langle\psi_{\text{gs}}| O_i^\dagger O_0 |\psi_{\text{gs}}\rangle,$$

for which δ-peaks signal the presence of long-range order in the ground state (the wave vector $\vec{q}$ determines the periodicity of the order).

More interesting are the dynamical properties of the system such as the dynamical correlation function

$$C(i,t) = \langle A_i(t) A_0(0)\rangle$$

with $A_i(t) = \mathrm{e}^{iHt} A_i \mathrm{e}^{-iHt}$ the operator A working at site i, time-evolved in the Heisenberg picture. Upon Fourier transforming this space-time correlation function, we obtain the frequency-momentum resolved dynamical correlation function or spectral function $S(\vec{q},\omega)$

$$S(\vec{q},\omega) = \sum_{i\in\mathcal{L}} \int_{-\infty}^{+\infty} \mathrm{d}t\ C(i,t) \mathrm{e}^{-i(\vec{q}\cdot\vec{n}_i - \omega t)}.$$

This spectral function[6] can be rewritten as

$$\begin{aligned} S(\vec{q},\omega) &= \sum_{i\in\mathcal{L}} \int_{-\infty}^{+\infty} \mathrm{d}t\ \mathrm{e}^{-i\vec{q}\cdot\vec{n}_i} \mathrm{e}^{i\omega t} \langle\psi_{\text{gs}}| \mathrm{e}^{iHt} A_i \mathrm{e}^{-iHt} \left(\sum_\alpha |\alpha\rangle\langle\alpha|\right) A_0(0) |\psi_{\text{gs}}\rangle \\ &= \sum_\alpha \left|\langle\alpha| A(\vec{q}) |\psi_{\text{gs}}\rangle\right|^2 2\pi\delta(\omega - E_\alpha) \end{aligned} \tag{2.1}$$

where $\sum_\alpha$ represents a sum over all excited states of the system with excitation energies E_α and $A(\vec{q}) = \sum_{i\in\mathcal{L}} \mathrm{e}^{i\vec{q}\cdot\vec{n}_i} A_i$. Typically, the operator A will only excite the first low-lying states, so that the spectral function essentially contains the momentum-frequency resolved information on the low-lying excitation spectrum of the system. A crucial observable is the gap Δ, the energy difference between the ground state and the first excited state, such that $S(\vec{q},\omega) = 0$ if $\omega < \Delta$. In the case of periodic boundary conditions and a translation-invariant Hamiltonian, all excited states can be

[6] Note that the static structure factor is regained from the dynamic correlations as

$$s(\vec{q}) = \int \mathrm{d}\omega\ S(\vec{q},\omega).$$

labeled by a momentum quantum number $\vec{p}$, defined as the phase of the eigenvalue of the translation operator $T_{\vec{e}}$

$$T_{\vec{e}}|\vec{p}\rangle = \mathrm{e}^{i\vec{p}\cdot\vec{e}}|\vec{p}\rangle.$$

Typically, a Hamiltonian has a few low-lying momentum-energy curves in its excitation spectrum; one such curve is often interpreted as a particle with a characteristic dispersion relation.[7]

Another set of observables is related to the sudden application of non-local perturbations to the system. Suppose we apply an external time- and space-dependent perturbation $h(i,t)$ that couples to the operator A at site i, such that the Hamiltonian changes abruptly as

$$H \to H - \sum_{i\in\mathcal{L}} h(i,t)A_i.$$

The shift away from the ground state value for a given observable O at site i is given by

$$\delta\langle O_i\rangle(t) = \sum_{j\in\mathcal{L}} \int_{-\infty}^{+\infty} \mathrm{d}t'\ \chi(\vec{n}_i - \vec{n}_j, t-t')h(j,t'),$$

where the dynamic susceptibility $\chi(\vec{n},t)$ characterizes the response of the system. Again, it is most interesting to consider the momentum-frequency resolved version,

$$\chi(\vec{q},\omega) = \sum_{i\in\mathcal{L}} \int_0^{\infty} \mathrm{d}t\ \mathrm{e}^{-i(\vec{q}\cdot\vec{n}_i-\omega t)}\chi(\vec{n}_i,t).$$

Interestingly, for $A = O$, the spectral function is related to the imaginary part of the susceptibility as ($\omega > 0$)

$$\mathrm{Im}\chi(\vec{q},\omega) = \frac{1-\mathrm{e}^{-\beta\omega}}{2} S(\vec{q},\omega),$$

in the regime where linear-response theory is valid.

2.1.4 *Quantum Phases and Phase Transitions*

One of the unifying goals of quantum many-body systems is the identification of all possible quantum phases of matter. A quantum phase is loosely defined as a collection of Hamiltonians, and corresponding ground states, that are all adiabatically connected, i.e. can be transformed into each other by a smooth interpolation of the parameters of the Hamiltonian without any drastic (non-analytic) changes in e.g.

[7] We refer to Chap. 3 for a worked-out version of the particle interpretation of elementary excitations.

the ground state energy. All ground states within the same phase have the same qualitative features such as similar correlation functions.

In contrast to classical phase transitions, a quantum phase transition [15] takes place at $T = 0$, and is driven by the competition between different terms in the Hamiltonian. In the Landau paradigm of phase transitions [16], a phase is characterized by the way the symmetries of the model are reflected in the ground state subspace and can be characterized by a local order parameter. As a phase transition is approached, the (quantum) fluctuations in this order parameter will diverge, explaining the system's non-analytic behaviour. The corresponding divergence of the correlation length ξ implies that there is no characteristic length scale in the system, giving rise to scale invariance.

The paradigmatic example of a second-order quantum phase transition is provided by the one-dimensional transverse-field Ising model [17], a chain of spins-1/2 with a Hamiltonian

$$H = -\sum_{\langle ij \rangle} \sigma_i^x \sigma_j^x - \lambda \sum_i \sigma_i^z,$$

where $\sum_{\langle ij \rangle}$ denotes a sum over nearest-neighbour pairs. At $\lambda = 1$, the model exhibits a phase transition between a single polarized state ($\lambda > 1$) and a twofold degenerate, ordered (i.e. symmetry-broken) ground state ($\lambda < 1$); the order parameter is $\langle \sigma^x \rangle$. This is reflected in the excitation spectrum as a closing of the gap at the transition; the new ground state that emerges after the transition point is formed as an extensive number of excitations have collapsed onto the old ground state. These vague notions will be made more precise in the following chapters.

Whereas the classical picture of Landau captures many second-order quantum phase transitions, a range of quantum phases has recently been discovered that cannot be characterized by any local order parameter. Indeed, these topological phases are characterized by global order parameters, related to long-range quantum correlations in the ground-state subspace – see Sect. 2.3.

2.1.5 The Link with Experiment

Although the problems that we try to solve have a clear mathematical meaning without any connection to an external reality, it is interesting to note that these simple many-body models can be realized in real-life experiments. In fact, the field of quantum many-body physics is characterized by a fruitful interplay between theory and experiment, so that a short overview of the experimental work is appropriate.[8]

[8] In the following chapters we will also mention a few experimental realizations of the specific models that we will study.

First of all, we have previously identified the Hubbard model as a paradigmatic example for theoretical strongly-correlated quantum physics, but the model seems to have experimental relevance as well. Indeed, in transition metal oxides the electrons are mostly localized around the lattice ions, and are at the same time interacting strongly. In these systems, metal-insulator phase transitions [18] can be observed [19]. The physics of the Hubbard model has received increased attention as it might explain the origin of high-T_c superconductivity [20].

Quantum spin systems can be realized in a number of different compounds [21], but in order to display non-trivial quantum physics, these systems should have a reduced dimensionality and/or frustrated interactions; in this way, a non-classical many-body state can be a stable ground state at $T \to 0$. The thermodynamic properties such as the magnetic susceptibility and the specific heat can be measured, and using e.g. inelastic neutron scattering [22] the spectral function can be probed directly.[9]

Recently, elementary quantum many-body models were artificially realized in experiments with ultracold gases. After the experimental realization of Bose–Einstein condensation [24, 25] in 1995, a new research field of artificially creating strongly-correlated quantum many-body physics has emerged [26–28]. Famously, the quantum phase transition of a bosonic gas in a lattice between a superfluid and a Mott insulator, as proposed theoretically [29, 30], was observed in the lab [31], as well as the one-dimensional Tonks–Girardeau gas [32–34] or quantum spin models [35, 36]. Alternatively, the ideas of using trapped ions [37] to simulate quantum spin models [38], or photons [39] to study e.g. entanglement in spin systems [40] have been implemented.

The overarching theme and goal in these recent developments is the realization of a universal quantum simulator [41, 42], a device that can simulate the quantum behaviour of generic many-body systems [43]. Part of the motivation for this line of research is the development of a universal quantum computer that would realize an immense speed-up for certain computational tasks as compared to classical computers [44].

2.2 Entanglement in the Low-Energy Subspace

The fundamental ingredient that characterizes a quantum-mechanical treatment of a many-body system is entanglement; it is because spins are entangled in a quantum-mechanical ground state that they can have non-trivial correlations even at temperature zero. Moreover, it is through entanglement that phenomena such as quantum phase transitions [46, 200] and topological order can exist [47–49]. From this perspective, it is crucial to have a clear understanding of how entanglement is distributed in a physical system. Nonetheless, it is only recently that the study of entanglement – originally the subject of quantum information theory, where entanglement has been

[9] We refer to Ref. [23] for all details on magnetic materials.

studied as a resource for non-classical computation [44, 50] – has found its way in quantum many-body physics [51] and has led to a number of great advances in both theoretical understanding and numerical simulation.[10]

The first step is taken by quantifying entanglement in a many-body state. The idea is that we take a state of a large system, define the reduced density matrix ρ_A of a small region A by tracing over all the other spins in the lattice, and compute the Von Neumann entropy associated with this density matrix as

$$S(\rho_A) = -\mathrm{Tr}\,(\rho_A \log \rho_A)\,.$$

This quantity expresses the amount of quantum correlations between region A and its environment. If the region is completely uncorrelated with its environment, the entanglement entropy is zero. For generic quantum states, where every spin is correlated with every other spin, the entanglement scales with the size of the considered region – as one would expect for an entropy measure.

For the low-energy states of physical systems, one expects that neither of these scenarios will be realized; the system's interactions will generate some quantum correlations but, because the interactions are local, entanglement will not spread out through the system over arbitrary distances. In fact, it has been observed that the entanglement entropy for low-energy states of local Hamiltonians typically scales as the perimeter of the considered region, instead of the volume. This *area law* of entanglement entropy [53] has led to the realization that the entanglement in physical states is distributed in a special way, and that a clear understanding of the entanglement structure is crucial for solving the quantum many-body problem.

In fact, many properties of ground states of local Hamiltonians have been rigorously proven. These proofs often start from Lieb–Robinson bounds [54], which state that the speed of information propagation in quantum spin systems is bounded by some characteristic velocity. These bounds play the role that strict causality plays in relativistic quantum field theory, and allow to translate results from relativistic quantum field theory to the setting of quantum lattice systems. One such result is that the ground state of a gapped local Hamiltonian has exponential decay of correlations [55], i.e.

$$|\langle O_A O_B\rangle - \langle O_A\rangle\langle O_B\rangle| < \mathrm{e}^{-d(A,B)/\xi}$$

where $d(A, B)$ is the distance between the operators O_A and O_B acting on separate regions A and B. This stands in contrast to critical models, where the ground state correlations generically decay algebraically with the distance.

Although the area law for the entanglement entropy is believed to be valid for all gapped systems, this has only been rigorously proven in one dimension. There it has been shown [56] that the entanglement entropy of a region is bounded – the area of a one-dimensional region is a constant – for ground states of gapped systems. For critical one-dimensional ground states, it scales logarithmically with the size of the subsystem (which is still very small compared to arbitrary quantum states), as

[10] The results mentioned in this section are laid out in exquisite detail in Ref. [52].

suggested by conformal field theory [57]. For higher-dimensional system, no rigorous results have been obtained with the same generality.

The proof of the area law for gapped one-dimensional systems confirmed the belief that their ground states can be approximated by matrix product states [56, 58], a class of states with a number of parameters that scales polynomially with the size of the system – see Sect. 2.6. Moreover, it is guaranteed that this approximation can also be found with a polynomial-time algorithm [59]. These results imply that the classical simulation of quantum many-body system is not impossible, but does require that entanglement is treated in an efficient way.

2.3 Low-Dimensional Quantum Physics

This work is focused on the low-energy physics of quantum systems of reduced dimensionality for two reasons: (i) the methods that we develop only work for this low-dimensional setting, and (ii) low-dimensional quantum matter can exhibit physical phenomena that are not observed for their three-dimensional counterparts. Whereas the former is of course not an argument for studying these systems, in this section we will argue for the latter and show why low-dimensional quantum physics is worth considering.

A first point in case is the fact that quantum correlations are stronger in lower-dimensional settings. The reason is the so-called monogamy property of entanglement [60, 61], implying that there is a limited resource of entanglement that a quantum degree of freedom can share with other ones. In particular, if a qubit A is maximally entangled with B, it can not be entangled with a third party C. In an extended quantum spin system, every spin will try to spread its limited amount of entanglement in an optimal way with all neighbouring spins, leading to strongly-correlated states. Now the number of neighbours clearly depends on the coordination number and dimensionality of the lattice; the entanglement will be strongest in low-dimensional lattices. On the other hand, in the limit for infinite-dimensional lattices where every spin has an infinite number of neighbours, the ground state of a translation-invariant model will have no entanglement at all and mean-field theory can be safely applied.

A second important result is the Mermin–Wagner theorem [62, 63], stating that one- and two-dimensional systems of statistical mechanics do not break continuous symmetries at finite temperature. The quantum version of this theorem was proven by Coleman [64], and states that one-dimensional quantum systems do not break continuous symmetries, even at zero temperature. The physical reason is that, if such a symmetry would be broken, the resulting Goldstone bosons would restore this symmetry due to the strong quantum fluctuations in one dimension. These results imply that low-dimensional systems have a stronger tendency to be disordered, i.e. no long-range order will develop because of strong quantum ($T = 0$) or thermal ($T > 0$) fluctuations.

The Heisenberg antiferromagnet serves as the best example to illustrate the effects of dimensionality. Classically (in a bipartite lattice, where classical frustration is absent), the ground state is the Néel state, where every spin is anti-aligned with all its

nearest neighbours. This staggered magnetization survives on the two-dimensional square lattice at zero temperature, although it is highly suppressed by quantum fluctuations; any finite temperature immediately destroys long-range order [65, 66]. For the one-dimensional chain, the Néel order is completely destroyed by quantum fluctuations and the ground state is disordered [67, 68].

This picture can be understood from spin-wave theory [69, 70], a third way to illustrate the connection between dimensionality and quantum fluctuations. The idea is to perturb from the large-s limit where the spins become essentially classic, and look at (quantum) $1/s$ perturbations in terms of "spin waves". To this end the model is mapped to an effective boson model by the Holstein–Primakoff transformation [71]

$$S^+ = \left(\sqrt{2s - b^\dagger b}\right) b, \qquad S^- = b^\dagger \left(\sqrt{2s - b^\dagger b}\right), \qquad S^z = s - b^\dagger b.$$

The square-root factors can be expanded in $1/s$, such that the Heisenberg interaction ($J > 0$) is written as a bosonic Hamiltonian

$$H = -\frac{|\mathcal{L}|}{2} J s^2 z + J s z \sum_{\vec{k}} \left(b^\dagger_{\vec{k}} b_{\vec{k}} + \frac{\gamma_{\vec{k}}}{2} \left(b^\dagger_{\vec{k}} b^\dagger_{-\vec{k}} + b_{\vec{k}} b_{-\vec{k}} \right) \right) + \dots$$

with $\gamma_{\vec{k}} = \sum_{\langle ij \rangle} \mathrm{e}^{i\vec{k}\cdot(\vec{n}_i - \vec{n}_j)}$ and z the coordination number of the lattice; the dots represent higher order terms in $1/s$ such as quartic terms in the bosonic operators, representing spin wave interactions [72]. The quadratic part is readily solved by a Bogoliubov transformation, yielding the spin-wave spectrum

$$\omega(\vec{k}) = J s z \sqrt{1 - \gamma^2_{\vec{k}}}.$$

In the case of a cubic lattice in any dimension, the spectrum becomes gapless around the points $\vec{k} = 0$ and $\vec{k} = \vec{\pi}$ with a linear dispersion. The Bogoliubov transformation introduces Holstein–Primakoff bosons in the ground state, which reduces the zero-temperature Néel order of the antiferromagnet. In fact, the zero'th-order correction to the staggered magnetization upon the classical Néel ground state diverges in one dimension for every value of s, whereas, in two dimensions, it diverges at finite temperature. In correspondence with the Mermin–Wagner theorem, it is the long wavelength or low-energy ($\omega(\vec{k}) \to 0$) modes that destroy the long-range order.

2.3.1 One Dimension

In one dimension, quantum fluctuations and disorder are strongest, which makes them exhibit unexpected quantum phenomena. Let us review the most important results.[11]

[11] See also Ref. [73].

Interestingly, a number of analytic results are known for one-dimensional quantum systems. The first one is the Lieb–Schultz–Mattis theorem [74], stating that the spin-s Heisenberg chain is gapless if s is half-integer. This result was extended [75] to the claim that basically any reasonable local Hamiltonian for a half-integer spin chain either has a unique ground state with gapless excitations or degenerate symmetry-broken ground states.

The theorem does not make any predictions on the case of integer spin, and, in fact, it appears that the opposite is true. It was Haldane [76, 77] who first made the conjecture that generic Hamiltonians for integer-spin models have a unique ground state with a gap to the first excited state that survives in the thermodynamic limit. The conjecture was based on a mapping of the Heisenberg model onto the non-linear sigma model, which captures the long-wavelength behaviour of the Heisenberg model for large spin but remains qualitatively correct for small spin as well [78]. Although the conjecture came as a shock initially, soon a spin-1 chain model was introduced [79, 80] for which an excitation gap can be proven, and numerical simulations quickly settled the issue in favour of a gap for the spin-1 Heisenberg model as well [81].

A third result that has shaped the physics of one-dimensional quantum systems is the Luttinger-liquid concept [73, 82, 83], which provides a phenomenological description of the low-energy excitations of critical one-dimensional quantum liquids [84, 85] and spin chains [86]. It maps these systems onto the Tomonaga–Luttinger model [87, 88], a model for describing a gas of electrons with a linear dispersion, which can be exactly solved by bosonization even in the presence of density-density interactions. This universal mapping implies that any critical quantum system in one dimension has an excitation spectrum consisting of bosonic density waves with a linear spectrum, and different correlation functions have a universal form depending on essentially two parameters [73].

Finally, the presence of a number of non-trivial symmetries and conserved quantities has dramatic effects on the physics of the class of integrable [Sect. 2.5] and/or conformal models [73, 89]. Whereas the former give rise to the absence of thermalization or ballistic transport, a conformal symmetry has great implications on the correlations and excitations of critical systems.

These results have led to a unified understanding of the physics of one-dimensional quantum systems in terms of the elementary excitations. Still, there is an extremely rich variety in the properties of these excitations that can be traced back to a purely quantum-mechanical origin. One important point is that elementary excitations can have non-trivial topological properties, a feature that was observed e.g. in the spin-1/2 Heisenberg model [90] where the elementary excitations can only be created in pairs because of their topological nature. In addition, elementary excitations in one dimension often have fractionalized quantum numbers, which points again to their collective nature. A third characteristic is that the statistics of the excitations or quasiparticles is not very well-defined [91], as it is impossible to clearly isolate a particle's statistics from its interactions and topological properties. This has led to the realization that bosonic and fermionic descriptions often lead to complementary descriptions of the same physics, and that mappings between the two can give additional physical insights [92].

We refer to Chaps. 3 and 4 for a more detailed and idiosyncratic view on the physics of one-dimensional quantum systems, and, in particular, the properties of elementary excitations.

2.3.2 Two Dimensions

Whereas the Heisenberg antiferromagnet on the square lattice develops long-range order in the ground state and can be treated, at least qualitatively, using spin-wave theory, in the last years a range of two-dimensional models have been show to remain disordered at zero temperature. These so-called quantum spin liquids [93–95] exhibit massive amounts of entanglement and, therefore, cannot be connected to any classical phase of matter. The easiest way to construct a quantum spin liquid is in terms of valence bonds, i.e. pairs of spins that form maximally entangled singlet states. If all spins are partitioned in specific valence bonds – a so-called valence bond solid or crystal – the system is non-magnetic. It does break translational symmetry, however, and has no long-range entanglement, so these states cannot be true quantum spin liquids. Instead, we should allow for quantum fluctuations between different valence bond configurations, giving rise to a resonating valence-bond state [96, 97]. These states restore all symmetries and exhibit long-range entanglement. They (possibly) appear as ground states of quite simple model Hamiltonians such as the nearest-neighbour antiferromagnet on the kagomé lattice [98–100] or the next-nearest-neighbour antiferromagnet on the triangular lattice [101, 102]. Interestingly, quantum spin liquids typically support excitations with fractional quantum numbers, pictured as localized excitations with a non-local string running through the lattice. These strings correspond to local rearrangements of the spins and have no associated energy cost, and imply that the excitations can have non-local properties.

The second reason for studying two-dimensional quantum physics is the observation of phases of matter that are not detectable by any local order parameter, but are instead characterized by topological order [103, 104]. Although this concept is lacking a clear-cut definition, topologically ordered systems have a few characteristic properties [104] such as (i) a ground-state degeneracy depending on the topology of the surface on which it is defined [105], (ii) emergent quasiparticle excitations with anyonic statistics [106–109] (iii) gapless boundary excitations [110–112], and (iv) the presence of long-range entanglement in the ground state [47, 48]. Topological order is realized in fractional quantum Hall states, which appear as ground states of two-dimensional electrons under strong magnetic fields [113, 114], and has recently attracted a lot of attention as it might be used as a resource for quantum memories [115] and computations [116].

Gapped quantum spin liquids provide examples of topological order, so both phenomena are intimately connected; the unifying feature seems to be the non-trivial entanglement structure of two-dimensional quantum ground states. As we have seen, the study of entanglement in many-body physics is a relatively new topic, so that

its theoretical understanding is all but complete at this point. In addition, numerical techniques for capturing these exotic quantum phases are less developed than in one dimension, so that a lot of interesting physics remains unexplored.

2.4 Numerical Techniques

One of the most attractive features of the domain of quantum many-body physics is the interplay between analytic techniques and numerical simulations, an interplay that is deemed essential to obtain physical insight into quantum materials. The numerical techniques that have dominated twentieth-century physics and that are based on mean-field techniques or independent particle models – think of Hartree–Fock [117–119] and density functional theory [120, 121] – are inaccurate for the purpose of simulating strongly-correlated systems. Moreover, since we are primarily interested in quantum phases that are not connected to some trivial (classical or free) limit, it seems that all standard forms of perturbation theory such as diagrammatic techniques [122] are excluded. In this section we briefly review some numerical algorithms that *can* capture strong quantum correlations in order to know what the methods of this dissertation are competing against.

The most obvious method for capturing the low-energy physics of simple models is by numerically diagonalizing the Hamiltonian on small system sizes, a method known as exact diagonalization [123, 124]. At low temperatures the interest is only in the low-energy states, such that only a small number of extremal eigenvalues and eigenvectors is wanted; in that case, iterative eigensolvers with fast convergence properties such as the Lanczos algorithm [125] can be applied. The major drawback of the method is the exponential scaling of the Hilbert space as a function of system size; for a system of N spins with d internal levels, the size of the Hilbert space is d^N. This complexity can be scaled down significantly by exploiting physical symmetries, but even then the present-day limit seems to be around 40-50 sites (in the case of a spin-1/2 model) [126].

Larger systems can be simulated using quantum Monte Carlo methods, based on the Monte Carlo technique [127] for simulating systems of classical statistical mechanics. As the original method is based on sampling a probability distribution, the challenge for quantum Monte Carlo is to map a quantum-mechanical problem to a representation with probabilistic interpretation. A popular approach is based on a stochastic series expansion [128], an expansion of the partition function in powers of inverse temperature and in "operator strings". In all quantum Monte Carlo methods, these mappings can lead to negative signs in the probability distributions, which can be formally circumvented, but lead to large errors for large system sizes and low temperatures. In special cases, this sign problem [129] can be eliminated, but for generic quantum systems with frustration or fermions, it appears to be an insurmountable obstacle for any quantum Monte Carlo approach.

A third set of methods comprises of different perturbative series expansions [130], which allow to, starting from a certain well-understood limit, trace how properties

change under certain perturbations. A slightly different approach is a continuous unitary transformation [131–133], where a given Hamiltonian is continuously deformed into an effective model Hamiltonian for which the physical properties can be understood. As these methods are inherently perturbative, they are not well-suited to phase transitions or strongly-correlated phases that are not straightforwardly connected to a trivial limit.

Lastly, there is the variational approach to strongly-correlated quantum physics. In this approach, a variational wave function or ansatz is proposed for the ground state or low-lying excited states for a given model Hamiltonian, possibly with a number of variational parameters that can be numerically optimized. Famous examples of this approach include Hartree–Fock theory, for which the variational wave function is a Slater determinant [134, 135], the Gross–Pitaevskii equation for the interacting Bose gas [136, 137], the BCS theory of superconductivity [138, 139], the resonating valence bond state for two-dimensional antiferromagnets [96, 97], and the Laughlin wave function for the fractional quantum Hall effect [114]. Recently, the variational approach has been combined with quantum Monte Carlo techniques [140, 141], where a Gutzwiller-projected wave function is used to describe a quantum spin liquid [142]. In any case, the variational approach potentially works for every phase and has the advantage that it provides physical insight into the problem at hand, but, as it always involves an ansatz, the accuracy of the method is not completely under control.

2.5 Integrability and the Bethe Ansatz

In one-dimensional quantum many-body physics a special place is taken by the so-called integrable models [143–145]. These are discrete or continuous models for which the Hamiltonian has some special symmetry that allows to write down the exact ground state and excited states. The history goes back to Bethe's solution of the spin-1/2 Heisenberg chain [68], and later on the "Bethe ansatz" provided exact solutions of simple spin chain models such as the XXZ [146–148] and XYZ [149] chain, as well as the one-dimensional Hubbard model [8, 150] and the Lieb–Liniger gas [151, 152]. In this section we show how the coordinate Bethe ansatz works, and how it determines the low-energy spectrum. Afterwards, we explain how this spectrum is characterized and how the low-energy dynamics of an integrable model can be understood.

2.5.1 Solving the Heisenberg Model

Let us first follow the Bethe solution for the antiferromagnetic Heisenberg spin-1/2 chain, defined by the Hamiltonian

$$H = \sum_{n=1}^{N} \vec{S}_n \cdot \vec{S}_{n+1} = \sum_{n=1}^{N} \frac{1}{2} \left(S_n^+ S_{n+1}^- + S_n^- S_{n+1}^+ \right) + S_n^z S_{n+1}^z$$

where we identify the spins 1 and $N + 1$ (periodic boundary conditions). An obvious eigenstate is the spins-up state

$$|\Omega\rangle = |\ldots \uparrow \uparrow \uparrow \ldots\rangle$$

with an energy $E_\Omega = N/4$. Upon this reference state, we can now build magnon states, which are obtained by flipping one spin and making a momentum superposition

$$|1\rangle = \frac{1}{\sqrt{N}} \sum_{n=1}^{N} \mathrm{e}^{ipn} S_n^- |\Omega\rangle,$$

with dispersion relation

$$E(p) - E_\Omega = \cos p - 1.$$

Adding a second magnon is less straightforward because of the magnon-magnon interactions; generally, an eigenstate in the two-magnon sector can be written down as

$$|2\rangle = \sum_{n_1 < n_2 = 1}^{N} a(n_1, n_2) S_{n_1}^- S_{n_2}^- |\Omega\rangle,$$

The magnons only interact when they are on neighbouring sites, so let us take the following wave function for the two-magnon state

$$a(n_1, n_2) = \mathrm{e}^{ip_1 n_1} \mathrm{e}^{ip_2 n_2} + A(p_1, p_2) \mathrm{e}^{ip_2 n_1} \mathrm{e}^{ip_1 n_2},$$

which obeys the eigenvalue equation for $n_2 > n_1 + 1$ with an energy

$$E(p_1, p_2) - E_\Omega = (\cos(p_1) - 1) + (\cos(p_2) - 1).$$

When the particles are next to each other ($n_2 = n_1 + 1$), the eigenvalue equation reduces to

$$2\,[E - E_\Omega] a(n_1, n_2) = 2a(n_1, n_2) - a(n_1 - 1, n_2) - a(n_1, n_2 + 1),$$

or the equation for the coefficient $A(p_1, p_2)$

$$A(p_1, p_2) = -e^{i\theta} = -\frac{\mathrm{e}^{i(p_1 + p_2)} + 1 - 2\mathrm{e}^{ip_2}}{\mathrm{e}^{i(p_1 + p_2)} + 1 - 2\mathrm{e}^{ip_1}}.$$

This is a pure phase factor capturing the interactions between the magnons.

At this point, the boundary conditions are imposed. For the one-magnon state, the trivial condition $a(n+N) = a(n)$ leads to the momentum quantization

$$p = \frac{2\pi j}{N}, \qquad j = 0, \ldots, N-1.$$

For the two-magnon state the condition is $a(n_2, n_1 + N) = a(n_1, n_2)$, which results in

$$\begin{cases} -\mathrm{e}^{ip_1 N}\mathrm{e}^{i\theta} = 1 \\ \mathrm{e}^{ip_2 N} = -e^{i\theta} \end{cases} \quad \rightarrow \quad \begin{cases} Np_1 = 2\pi j_1 - \tilde{\theta}, & j_1 = 0, \ldots, N-1 \\ Np_2 = 2\pi j_2 + \tilde{\theta}, & j_2 = 0, \ldots, N-1 \end{cases}$$

with $\tilde{\theta} = \theta + \pi$. Through the non-trivial scattering phase $\theta(p_1, p_2)$, the magnon interactions determine the momentum quantization and, consequently, the energy of the two-magnon state.

Going to higher magnon numbers seems to be an intractable task, because a priori multi-particle scattering processes should be taken into account. It appears, however, that for this specific model, these processes always have zero amplitude and all magnon interactions can be decomposed into two-particle scattering processes, described by the two-magnon scattering phase shift $\theta(p_1, p_2)$. This implies that an M-magnon wave function can be written down explicitly as

$$|M\rangle = \sum_{n_1 < \cdots < n_M = 1}^{N} a(n_1, \ldots, n_M) S^-_{n_1} \ldots S^-_{n_M} |\Omega\rangle,$$

with the Bethe ansatz wave function for the coefficients

$$a(n_1, \ldots, n_M) = \sum_{\mathcal{P}} (-1)^{\mathcal{P}} \left(\prod_{\langle ij \rangle \in \mathcal{P}} \mathrm{e}^{i\theta(\lambda_i, \lambda_j)} \right) \mathrm{e}^{i\lambda_{\mathcal{P}(1)} n_1} \cdots \mathrm{e}^{i\lambda_{\mathcal{P}(M)} n_M},$$

where the sum runs over all permutations of the M different λ's. Again imposing periodic boundary conditions leads to the Bethe equations

$$\lambda_j = \frac{2\pi j}{N} - \frac{1}{N} \sum_{k=1}^{M} \theta(\lambda_j, \lambda_k),$$

for a set of integers $\{j\}$. It can be checked that this M-magnon state is indeed an eigenstate with an energy equal to the sum of the one-magnon energies

$$E(\lambda_1, \ldots, \lambda_M) = \sum_{j=1}^{M} (\cos(\lambda_j) - 1).$$

The ground state of the antiferromagnetic chain is obtained as the state with $N/2$ magnons; the corresponding Bethe equations can be solved numerically.

2.5.2 Coordinate Bethe Ansatz: General Set-Up

Let us take a more general perspective now: we consider a gas of one-dimensional bosons in the continuum that interact locally. The bosons have a dispersion relation $\epsilon_0(p)$, which is defined as the energy of one boson with momentum p in an infinite system. The only information on the interactions that is needed is the two-body S matrix $S(p_1, p_2)$, which can be defined as the coefficient that pops up in the asymptotic part of the stationary two-body wave function,[12]

$$\Psi_{p_1,p_2}(x_1, x_2) \to \mathrm{e}^{ip_1x_1}\mathrm{e}^{ip_2x_2} + S(p_1, p_2)\mathrm{e}^{ip_2x_1}\mathrm{e}^{ip_1x_2}, \qquad x_1 \ll x_2.$$

Based on this information, the coordinate Bethe ansatz wave function for a collection of N particles can be written down as

$$\Psi_{\{\lambda_i\}}(x_1, \ldots, x_N) = \sum_{\mathcal{P}} A(\mathcal{P})\mathrm{e}^{i(\lambda_{\mathcal{P}1}x_1+\cdots+\lambda_{\mathcal{P}N}x_N)}$$

where $\sum_{\mathcal{P}}$ is a sum over permutations of the λ's and $A(\mathcal{P})/A(\mathcal{P}') = S(\lambda_i, \lambda_j)$ if the permutations $\mathcal{P}$ and $\mathcal{P}'$ differ by the interchange of the momenta λ_i and λ_j. The wave function is determined by the set of N pseudo-momenta $\{\lambda_i\}$.

Imposing periodic boundary condition again leads to the Bethe equations

$$L\lambda_j + \sum_{k=1}^{N} \theta(\lambda_j, \lambda_k) = 2\pi n_j \qquad \forall j \tag{2.2}$$

where θ is the phase of the S-matrix, i.e. $S(\lambda_i, \lambda_j) = -\mathrm{e}^{i\theta(\lambda_i,\lambda_j)}$, and the n_j are (half) integers, depending on the number of particles being odd or even. Every solution of the Bethe equations is an eigenstate of our system and any eigenstate can be uniquely parametrized with a set of pseudo-momenta obeying Eq. (2.2). The total energy and momentum are given by

$$E_N = \sum_{j=1}^{N} \epsilon_0(\lambda_j) \qquad \text{and} \qquad P_N = \sum_{j=1}^{N} \lambda_j,$$

the sum of the bare energies and momenta. That the energy simply is the sum of the bare energies of all particles reflects the fact that all interactions have already been incorporated in the Bethe ansatz wave function. In fact, we do not even have to know how the particles interact or how the first-quantized Hamiltonian looks like; only

[12] This definition of the two-particle S matrix will be discussed in full detail in Chap. 3.

the one-particle dispersion and the two-particle S matrix are needed to extract all thermodynamic information about the system. The reason for this is of course that in an integrable system, the complete S matrix (three-, four-, …particle scattering) can be determined from the two-particle S matrix.

We now take the thermodynamic limit, i.e. we take $L, N \to \infty$ but keeping the density $D = N/L$ finite. The pseudo-momenta will form a dense set, so we define a density of pseudo-momenta $\rho(\lambda)$ describing a Fermi-sea filled up to a certain level q, such that $\rho(\lambda) = 0$ for $|\lambda| > q$. The Bethe equations are transformed into a linear integral for $\rho(\lambda)$ [151, 152]

$$\rho(\lambda) - \frac{1}{2\pi}\int_{-q}^{q} K(\lambda, \mu)\rho(\mu)\mathrm{d}\mu = \frac{1}{2\pi} \tag{2.3}$$

where the kernel of the integral equation is given by the derivative of the scattering phase, i.e. $K(\lambda, \mu) = \partial_\lambda \theta(\lambda, \mu)$. The Fermi level q is not known in advance; it is determined by the density as

$$D = \int_{-q}^{q} \rho(\lambda)\mathrm{d}\lambda.$$

When the density is not fixed, we have to implicitely determine the Fermi level q through the function $\epsilon(\lambda)$, the dressed energy of a pseudo-particle. This function obeys

$$\epsilon(\lambda) - \frac{1}{2\pi}\int_{-q}^{q} K(\lambda, \mu)\epsilon(\mu)\mathrm{d}\mu = \epsilon_0(\lambda).$$

The Fermi level q is determined by imposing that $\epsilon(q) = 0$, which implies that we have to solve the system for the function $\epsilon(\lambda)$ and the value for q, given a certain $\epsilon_0(\lambda)$ self-consistently.

Elementary excitations are easily characterized in terms of the pseudo-particles of the Bethe ansatz. We can construct two types of excitations: either we take one particle with momentum $|\lambda| < q$ out of the Fermi sea (hole excitation) or we add one particle with momentum $|\lambda| > q$ (particle excitation). The energy of these excitations has two contributions: the bare energy $\epsilon_0(\lambda)$ and the dressing from all the other particles. These two contributions are contained within the function $\epsilon(\lambda)$ so the energy of an excitation is given by the above equation. Analogously, the physical momentum of an excitation has two contributions:

$$p(\lambda) = \pm\lambda \pm \int_{-q}^{q} \theta(\lambda, \mu)\rho(\mu)\mathrm{d}\mu \tag{2.4}$$

where the plus, resp. minus, sign is for a particle, resp. hole. Here it is assumed that λ is the bare momentum of the particle.

2.5.3 Thermodynamic Bethe Ansatz

At zero temperature, the coordinate Bethe ansatz describes an integrable system in its ground state by filling up a Fermi sea of quasi-momentum states; its excitations are holes and particles above this Fermi sea. When a finite temperature T is applied, these particles and holes will have finite distribution densities. By associating an entropy to these distributions and minimizing the free energy, one arrives at the Yang–Yang equation [153]

$$\epsilon(\lambda) = \epsilon_0(\lambda) - \frac{T}{2\pi}\int_{-\infty}^{+\infty} K(\lambda,\mu)\ln\left(1+\mathrm{e}^{-\epsilon(\mu)/T}\right)\mathrm{d}\mu,$$

a non-linear integral equation for the dressed energy $\epsilon(\lambda)$ of the quasi momentum states; the equation can be solved by iteration [154]. The density of occupied vacancies $\rho(\lambda)$ is given by

$$\theta(\lambda) = \frac{\rho(\lambda)}{\rho_v(\lambda)} = \frac{1}{1+\mathrm{e}^{\epsilon(\lambda)/T}}$$

with $\rho_v(\lambda)$ the density of all (occupied and empty) vacancies. Through this equation the density of occupied vacancies satisfies the integral equation

$$\rho(\lambda) = \frac{\theta(\lambda)}{2\pi}\left(1+\int_{-\infty}^{+\infty} K(\lambda,\mu)\rho(\mu)\mathrm{d}\mu\right),$$

such that the total density can be calculated as

$$D = \int_{-\infty}^{+\infty}\rho(\lambda)\mathrm{d}\lambda.$$

2.5.4 Dynamics and Out-of-Equilibrium

If one wishes to extract the physical properties of integrable systems the construction of the ground state is only the first step. Due to the special symmetries of integrable systems, however, the low-energy spectrum has an equally special structure. Indeed, due to the particular conservation laws in integrable models, the elementary excitations can be treated as "particles" scattering off each other according to two-body S matrices, where all particle production processes are absent and particle number is conserved [155].

S Matrix and Faddeev–Zamolodchikov Algebra

We can describe this low-lying spectrum formally with the so-called Faddeev-Zamolodchikov operators [155–157], that create the exact elementary excitations out of the ground state $|\psi_{\mathrm{gs}}\rangle$ of the interacting theory:

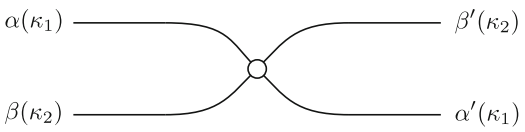

Fig. 2.1 Graphical representation of the two-particle S matrix $S_{\alpha\beta}^{\alpha'\beta'}(\kappa_1, \kappa_2)$. Momentum and energy conservation in one dimension imply that the outgoing momenta are equal to the incoming ones

$$|\kappa\rangle_\alpha = Z_\alpha^\dagger(\kappa)|\psi_{\mathrm{gs}}\rangle$$

where $|\kappa_\alpha\rangle$ is an elementary excitation of type α with momentum κ. The S matrix $S_{\alpha\beta}^{\alpha'\beta'}(\kappa_1, \kappa_2)$ describes the scattering amplitude and phase for the process where two particles $\{\alpha, \beta\}$ with momenta κ_1 and κ_2 scatter into two, potentially different, particles $\{\alpha', \beta'\}$ (the individual momenta are preserved); it is visualized in Fig. 2.1. The S matrix determines the commutation relations of the Faddeev-Zamolodchikov operators

$$\begin{aligned}
Z_\alpha(\kappa_1)Z_\beta(\kappa_2) &= S_{\alpha\beta}^{\alpha'\beta'}(\kappa_1, \kappa_2)Z_{\beta'}(\kappa_2)Z_{\alpha'}(\kappa_1)\\
Z_\alpha^\dagger(\kappa_1)Z_\beta^\dagger(\kappa_2) &= S_{\alpha\beta}^{\alpha'\beta'}(\kappa_1, \kappa_2)Z_{\beta'}^\dagger(\kappa_2)Z_{\alpha'}^\dagger(\kappa_1)\\
Z_\alpha(\kappa_1)Z_\beta^\dagger(\kappa_2) &= 2\pi\delta(\kappa_1 - \kappa_2)\delta_{\alpha\beta} + S_{\beta\alpha'}^{\beta'\alpha}(\kappa_1, \kappa_2)Z_{\beta'}^\dagger(\kappa_2)Z_{\alpha'}(\kappa_1).
\end{aligned}$$

The hallmark of integrability now is the fact that all scattering processes can be decomposed into two-particle processes described by the two-particle S matrix $S_{\alpha\beta}^{\alpha'\beta'}(\kappa_1, \kappa_2)$. The three-body S matrix is decomposed into consecutive two-body S matrices in two ways [see Fig. 2.2]

$$\begin{aligned}
S_{\alpha\beta\gamma}^{\alpha'\beta'\gamma'}(\kappa_1, \kappa_2, \kappa_3) &= S_{\alpha\beta}^{ij}(\kappa_1, \kappa_2)S_{i\gamma}^{\alpha'k}(\kappa_1, \kappa_3)S_{jk}^{\beta'\gamma'}(\kappa_2, \kappa_3)\\
&= S_{\beta\gamma}^{jk}(\kappa_2, \kappa_3)S_{\alpha k}^{i\gamma'}(\kappa_1, \kappa_3)S_{ij}^{\alpha'\beta'}(\kappa_1, \kappa_2).
\end{aligned}$$

These two decompositions should be equal, which leads to a consistency condition on the two-body S matrix; this equation is called the Yang–Baxter equation [149, 158]. This elastic scattering implies that all low-lying excitations of the fully-interacting system can be pictured as many-particle states on top of the strongly-correlated ground state. Labelling these states by their particle numbers, all low-lying states are created by the Faddeev-Zamolodchikov operators as

$$|\kappa_1, \ldots, \kappa_m\rangle_{\alpha_1,\ldots,\alpha_m} = Z_{\alpha_1}^\dagger(\kappa_1)\ldots Z_{\alpha_m}^\dagger(\kappa_m)|\psi_{\mathrm{gs}}\rangle.$$

Dynamical Correlations

This structure of the low-lying spectrum can be used to compute dynamical correlation functions or spectral functions of integrable systems. We have seen [Eq. (2.1)]

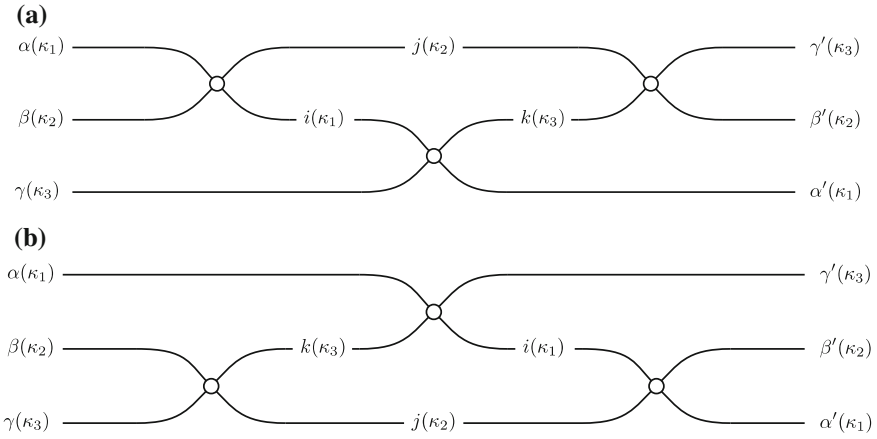

Fig. 2.2 Two ways in which the three-particle S matrix $S_{\alpha\beta\gamma}^{\alpha'\beta'\gamma'}(\kappa_1, \kappa_2, \kappa_3)$ can be decomposed in two-particle scattering processes

that the spectral function can be written as a sum of matrix elements of local operators in the eigenstate basis (form factors). The computation is, because of the unwieldy form of the Bethe ansatz wave functions, a rather tedious task, but a lot of progress has been made recently [159–162]. The success of this approach is explained by the fact that it is only the few-particle excitations (as created by the FZ operators) that contribute to the low-energy spectral functions. For a gapped system this is obvious: because every particle carries a minimum energy of Δ (the gap), an m-particle state has an energy larger than $m\Delta$. At low enough energies, only a few particles will contribute to the spectral function and it can be computed exactly by summing over all of them. Even for critical models, the spectral weight in higher-particle states seems to decrease rapidly.

For the case of gapped systems, this same approach can be applied to the computation of dynamical correlation functions at finite temperature [155, 163–168]. Indeed, the factor $\mathrm{e}^{-n\Delta/T}$ provides a suppression factor for the contribution of n-particle states, which allows for an efficient summation of the form factors at low enough temperatures.

Real-Time Evolution

The absence of three-particle scattering has another interesting consequence in the behaviour of integrable systems out of equilibrium. Since the ground-breaking "quantum Newton's cradle" experiment, showing the absence of thermalization of a quasi one-dimensional many-body system [34], there has been a number of theoretical studies on the effect of integrability on thermalization processes. In particular, it has been shown that, instead of relaxing to a thermal Gibbs ensemble, integrable systems relax to a so-called generalized Gibbs ensemble [169–171]. The reason is that integrable systems have, in addition to the energy, an extensive number of local [143] or quasi-local [172, 173] conserved quantities $\{I_m\}$ that determine the reduced density matrix at infinite times as

$$\rho_{\mathrm{GGE}} = \frac{1}{Z} \exp\left(- \sum_m \lambda_m I_m \right),$$

similar to the way in which ensembles are constructed in statistical mechanics [174, 175].

We can again make sense of this in terms of the particle structure of the low-lying excitations and the Faddeev-Zamolodchikov operators. Indeed, because they correspond to exact excitations of the fully-interacting Hamiltonian and they are preserved in all scattering processes, the particle numbers

$$N_\alpha(\kappa) = Z_\alpha^\dagger(\kappa) Z_\alpha(\kappa)$$

are integrals of motion, such that a representation of the generalized Gibbs ensemble can be written down in terms of them [176–178]. In the case of free theories, quenching from the one Hamiltonian to the other amounts to doing a Bogoliubov rotation in the space of the particle creation operators, such that the particle occupation numbers $n_\alpha(\kappa) = \langle N_\alpha(\kappa) \rangle$ can be computed exactly [179]. In the case of interacting integrable models, this approach seems to be harder to follow through [180].

Another approach for constructing the generalized Gibbs ensemble is through the so-called generalized thermodynamic Bethe ansatz [181–183]. In this approach, the thermodynamic Bethe ansatz is extended to account for the additional conserved quantities. Again, in the thermodynamic limit one can find a "saddle-point" root density $\rho(\lambda)$ that describes the generalized Gibbs ensemble. Additionally, in Ref. [181] it was shown that a representative eigenstate $|\Phi_s\rangle$ can be found (i.e. go over to the micro-canonical ensemble) and that the dynamics at large enough times are determined by the non-extensive "excitations" on top of this state – these excitations can have positive and negative excitation energies, since the reference state is not the ground state. This implies that, for quenched integrable models, one has an excitation spectrum (with infinitely long-lived excitations) on top of the generalized Gibbs ensemble that determines the dynamics at long times. More specifically, one can observe the light-cone dynamics in quenched integrable models as a result of this quasiparticle spectrum [184].

2.5.5 *Breaking Integrability*

Although the Bethe ansatz gives rise to a number of concepts that are applicable to non-integrable one-dimensional systems as well – a large portion of this dissertation is a case in point – the question remains how generic the physics of integrability is for one-dimensional quantum many-body systems.

A number of studies has been performed that track the influence of small non-integrable terms in the Hamiltonian on the thermalization process. Between Hamiltonians far away from integrability, which seem to thermalize rather quickly, and

integrable ones, which don't thermalize at all, there seems to be a class of Hamiltonians with small non-integrable terms that lead to so-called prethermalization plateaux [179, 185–188]. These plateaux are characterized by a generalized Gibbs ensemble with the "almost" conserved quantities, and only after longer times do these systems relax to thermal Gibbs state.

2.6 Tensor Networks

In the last twenty-five years another set of methods was developed for simulating strongly-correlated quantum systems grouped under the name of "tensor network methods".[13] The unifying feature of these methods is their ability to capture the specific entanglement structure of low-energy states, and as such to provide an extremely accurate variational parametrization for describing and simulating quantum many-body physics. We have seen that quantum correlations in ground states of local Hamiltonians are distributed in a very special way, and the idea is to design a network of tensors that mimics this special distribution. In this way, tensor network states parametrize the "tiny corner of Hilbert space", where all the relevant physics is going on.

In order to see how a network of tensors can describe a many-body state, take a general state of N spins on an arbitrary lattice

$$|\Psi\rangle = \sum_{i_1,\ldots,i_N} c_{i_1,\ldots,i_N} |i_1, \ldots, i_N\rangle.$$

The coefficients $c_{i_1,\ldots,i_N}$ are complex numbers for every input of the indices; alternatively, they can be interpreted as defining a tensor with N indices. If we take the basis states $|i_1, \ldots, i_N\rangle$ as a given, we can say that the tensor describes the state. Graphically, the state can be depicted as

$|\Psi\rangle =$ 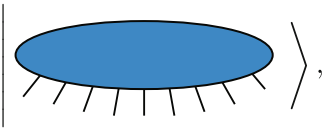 ,

where a geometric figure always represents a tensor with the legs corresponding to the tensor's indices. Now, a tensor network should be pictured as a decomposition of this one N-leg tensor as a contraction of a number of smaller tensors:

[13] This section should be more or less self-contained, but the reader is referred to review papers [189–191] for more details.

$$|\Psi\rangle_{\mathrm{TNS}} =$$ 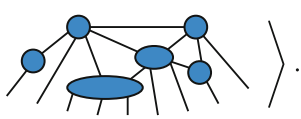 .

In this expression, we have introduced the graphical notation for a tensor network contraction: (i) whenever two tensors are connected, the connected indices are identified and summed over, and (ii) unconnected legs remain as indices of the resulting new tensor (if all legs are connected the diagram corresponds to a scalar). These graphical representations will be very useful throughout this dissertation.

The most important feature of tensor network states is that the dimensions of the virtual indices in these contractions will not be very large, so that the number of parameters that describe these states is small. This implies that such a low-rank tensor-network decomposition of a quantum state is generally not possible, but, of course, it will prove to be the case that tensor network states exactly target the low-energy subspace of physical systems. For the rest of this section, we will explain why different tensor networks indeed have the right entanglement properties and, most importantly, how this opens up the possibility to simulate strongly-correlated quantum many-body physics.

2.6.1 The Density-Matrix Renormalization Group

The story of tensor network states takes off with a few seemingly unrelated breakthroughs in different fields of physics; the first (not in a chronological sense) is the invention of the density-matrix renormalization group by S. White in 1992.

The first numerical implementation of the renormalization group was done by K. Wilson in his seminal work [192] on the Kondo problem. The Kondo model [193–195] describes a magnetic impurity coupled to the conduction band of a nonmagnetic metal; the crucial question, unsolvable by perturbation theory, is the low-temperature behaviour of this impurity spin. The idea of the numerical renormalization group [196] by Wilson is to (i) discretize the conduction band to discrete energy levels logarithmically, (ii) transform the system to a half-infinite spin chain with the first spin representing the impurity, and (iii) solving this spin-chain system iteratively. Starting from the impurity spin in every iteration a new degree of freedom is added to the system and, in order to keep the size of the Hilbert space tractable, the number of states is truncated by only keeping the lowest-energy states of the Hamiltonian for the current part of the chain.

The application of this numerical renormalization method to strongly-correlated spin chains proved to work rather poorly. White and Noack [197] showed that the truncation procedure of only keeping the low-energy states of a certain region of a spin chain is inaccurate for a real-space version of the renormalization group. Instead, White proposed [198, 199] to embed this region in a larger environment and use the

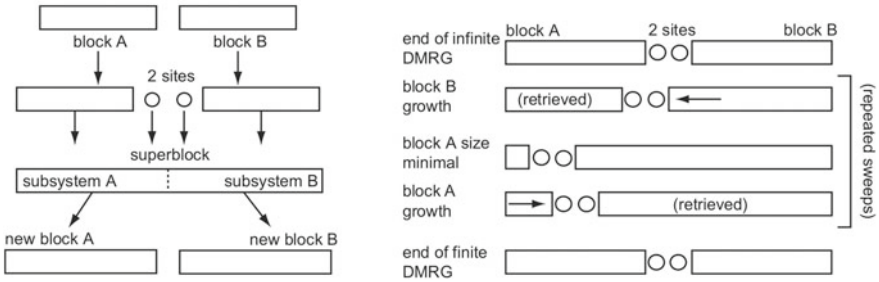

Fig. 2.3 Infinite-system (*left*) and finite-system (*right*) DMRG [201] (figure taken from Ref. [202]). In the infinite-system algorithm the system (block A) and the environment (block B) are grown by adding a site in every iteration. For the superblock the ground state $|\psi\rangle$ is found by a sparse eigensolver, after which a new reduced basis for block A is found by only keeping the m leading eigenvectors of the density matrix on block A, $\rho_A = \mathrm{Tr}_B(|\psi\rangle\langle\psi|)$; similarly for block B. The Hamiltonian and other observables are updated in every iteration by projecting on the kept subspace. The finite-system DMRG algorithm is applied to increase the accuracy: now the system size is kept to a fixed length L, and the growing of block A is at the cost of a shrinkage of block B and vice versa. The truncation procedure is only applied to the block that grows in size. If a boundary of the system is reached, the growing/shrinking is reversed. This algorithm converges to a good ground state after a number of "sweeps"

region's density matrix as the natural basis for truncating the number of states kept in every iteration. Suppose that the wave function of a block A and its environment E is given by ψ, and is approximated as $\tilde{\psi}$ by only keeping a basis of m states on the block A,

$$|\tilde{\psi}\rangle = \sum_{\alpha=1}^{m} \sum_{j=1}^{N_E} a_{\alpha j} |\alpha\rangle |j\rangle .$$

The error on the wave function $\epsilon = \| |\psi\rangle - |\tilde{\psi}\rangle \|$ is minimized by choosing the $|\alpha\rangle$ to be the eigenvectors corresponding to the m largest eigenvalues of the density matrix ρ_A, obtained by tracing out the environment degrees of freedom,

$$\rho_A = \mathrm{Tr}_E \left(|\psi\rangle\langle\psi| \right) .$$

This truncation scheme explicitly maximizes the entanglement between the block A and its environment [45, 200]. This interpretation reveils the basic motive of the DMRG prodecure as shifting the renormalization flow towards the entanglement degrees of freedom, instead of the original energy/momentum rescaling of Wilson.

The success of DMRG was immediate; a first illustration of its accuracy was given in Ref. [203] where the ground-state energy of the spin-1 Heisenberg antiferromagnet was calculated at almost machine precision, whereas the Haldane gap [Sect. 2.3] was estimated with an accuracy of five digits. In the following years, DMRG has

evolved in the standard for obtaining static properties of one-dimensional quantum lattice models [204, 205] – in Fig. 2.3 the general strategy of DMRG is presented schematically.

Yet, the success of DMRG has for a long time been something of a miracle; its power for simulating quantum spin chains has only been fully understood by identifying it as a variational method that optimizes over a specific class of tensor network states. Indeed, it was realized [206–208] that the finite-system DMRG algorithm leads to a ground state in the form of a *matrix product state*. Only some years later this development was taken seriously and the power of matrix product states investigated systematically. As a result, it was understood how DMRG efficiently captures the entanglement distribution in one-dimensional quantum lattice models and in what ways DMRG can be extended in order to capture e.g. dynamical and finite-temperature behaviour [202, 209].

2.6.2 *Finitely Correlated States*

A few years before the conception of DMRG, however, matrix product states had already appeared under the name of valence bond solids or finitely correlated states.

The former were introduced by Affleck, Kennedy Lieb and Tasaki (AKLT) in 1987 [79, 80] as a class of translation-invariant quantum states with exponential decay of correlations. They generalized the work of Majumdar and Ghosh [210–212], who showed that the two states with purely nearest-neighbour valence bonds are the exact ground states of the spin-1/2 antiferromagnet with equal nearest-neighbour and next-nearest-neighbour coupling. From such a dimerized state, a translation-invariant state is obtained by projecting spin-1/2 pairs onto the symmetric spin-1 subspace. The AKLT state on the spin-1 chain that is thus obtained has no broken symmetries and is the unique ground state of the simple Hamiltonian

$$H = \sum_i \left(\frac{1}{2}(\vec{S}_i \cdot \vec{S}_{i+1}) + \frac{1}{6}(\vec{S}_i \cdot \vec{S}_{i+1})^2 + \frac{1}{3} \right),$$

where every term is nothing more than a projector onto the spin-2 subspace of every nearest-neighbour pair of spins. In Ref. [80] it was also proven that this Hamiltonian has a finite excitation gap, a result that showed for the first time the existence of a gapped spin-1 antiferromagnet without broken symmetries in correspondence with Haldane's conjecture [Sect. 2.3]. The AKLT construction can be extended to higher spin models and higher dimensions, but the provability of the gap, although highly expected in some cases [see Sect. 5.6], is lost.

The one-dimensional AKLT state was later generalized [213] to the so-called finitely correlated states, a class of translation-invariant states for quantum spin chains in the thermodynamic limit. These states have, under some conditions, exponential decay of correlations and they are the ground states of local Hamiltonians with a finite gap.

In retrospect, finitely correlated states can be identified as uniform matrix product states in the thermodynamic limit, a class of states that will be extensively worked with in this dissertation. Although the use of finitely correlated states as variational trial states is already mentioned by the authors of Ref. [213], the connection with DMRG was, unfortunately, only noticed many years later. Also, it took another number of breakthroughs until the class of uniform matrix product states was used directly as a variational class for simulating spin chains in the thermodynamic limit directly.

2.6.3 Matrix Product States

Matrix product states (MPS) have appeared as subject of extensive research only in the years 2003–04, by the combination of ideas in quantum information theory and many-body physics. There are a few complementary ways of arriving at an MPS, all of which we will review in this section.

Construction of MPS

Consider a quantum state on a spin chain with N sites

$$|\Psi\rangle = \sum_{i_1,\ldots,i_N} c_{i_1,\ldots,i_N} |i_1, \ldots, i_N\rangle.$$

The number of coefficients $c_{i_1,\ldots,i_N}$ scales exponentially in the number of sites and provides a complete yet awkward parametrization of the state. The challenge is to find a representation that has a more local structure. Consider thereto a partition of the spin chain into two blocks A and B, with a corresponding Schmidt decomposition

$$|\Psi\rangle = \sum_{\alpha=1}^{D} \lambda_\alpha |\Phi_\alpha^A\rangle \otimes |\Phi_\alpha^B\rangle \tag{2.5}$$

where the Schmidt vectors $|\Phi_\alpha^{A,B}\rangle$ are orthonormal and the Schmidt numbers λ_α are arranged in decreasing order. The reduced density matrices on the two blocks are given by

$$\rho_{A/B} = \sum_{\alpha=1}^{D} \lambda_\alpha^2 |\Phi_\alpha^{A/B}\rangle\langle\Phi_\alpha^{A/B}|$$

such that the entanglement entropy between blocks A and B is given by

$$\begin{aligned} S_{A|B} &= -\mathrm{Tr}\,(\rho_A \log \rho_A) = -\mathrm{Tr}\,(\rho_B \log \rho_B) \\ &= -\sum_{\alpha=1}^{D} \lambda_\alpha^2 \log \lambda_\alpha^2. \end{aligned}$$

The advantage of the Schmidt decomposition is that the entanglement properties of low-energy states can be exploited: if the entanglement entropy of the region A is bounded, it is expected that the Schmidt spectrum falls off quickly and that the sum in Eq. (2.5) can be truncated efficiently. Indeed, an approximate wave function $|\tilde{\Psi}\rangle$ is obtained by only including the $D' < D$ leading Schmidt vectors, giving rise to a truncation error of

$$\| |\Psi\rangle - |\tilde{\Psi}\rangle \|^2 = \sum_{\alpha=D'+1}^{D} \lambda_\alpha^2. \tag{2.6}$$

Let us now use this Schmidt decomposition successively for all partitions of the spin chain [214, 215]. Isolating the first spin results in

$$|\Psi\rangle = \sum_{\alpha_1} \lambda_{\alpha_1} |\Phi_{\alpha_1}^{[1]}\rangle \otimes |\Phi_{\alpha_1}^{[2\ldots N]}\rangle = \sum_{i_1,\alpha_1} \Gamma_{\alpha_1}^{[1],i_1} \lambda_{\alpha_1} |i_1\rangle \otimes |\Phi_{\alpha_1}^{[2\ldots N]}\rangle,$$

where in the second step $|\Phi_{\alpha_1}^{[1]}\rangle$ was written out in the local spin basis $|i_1\rangle$. Next we make a partition after the second spin and apply the same procedure,

$$|\Psi\rangle = \sum_{i_1,\alpha_1} \sum_{i_2,\alpha_2} \Gamma_{\alpha_1}^{[1],i_1} \lambda_{\alpha_1} \Gamma_{\alpha_1,\alpha_2}^{[2],i_2} \lambda_{\alpha_2} |i_1, i_2\rangle \otimes |\Phi_{\alpha_2}^{[3\ldots N]}\rangle.$$

By iterating, the state is rewritten as

$$\begin{aligned} |\Psi\rangle &= \sum_{i_1,\ldots,i_N} \sum_{\alpha_1,\ldots,\alpha_{N-1}} \Gamma_{\alpha_1}^{[1],i_1} \lambda_{\alpha_1} \Gamma_{\alpha_1,\alpha_2}^{[2],i_2} \lambda_{\alpha_2} \ldots \Gamma_{\alpha_{N-2},\alpha_{N-1}}^{[N-1],i_{N-1}} \lambda_{\alpha_{N-1}} \Gamma_{\alpha_{N-1}}^{[N],i_N} |i_1, \ldots, i_N\rangle \\ &= \sum_{i_1,\ldots,i_N} \Gamma^{i_1}[1]\Lambda[1]\Gamma^{i_2}[2]\Lambda[2]\ldots\Gamma^{i_{N-1}}[N-1]\Lambda[N-1]\Gamma^{i_N}[N]|i_1,\ldots,i_N\rangle \end{aligned} \tag{2.7}$$

where the simplified notation was obtained by identifying the sums over indices as matrix multiplications and introducing the diagonal matrices $\Lambda[n]$. The matrices in this decomposition now have a physical interpretation: the Γ's describe some local description of the spin degrees of freedom, whereas the Λ's contain the Schmidt spectrum corresponding to a bipartition of the chain. An exact representation of any quantum state $|\Psi\rangle$ would require the size of these matrices to scale as $\mathcal{O}(\exp N)$, but for states with a bound on the bipartite entanglement entropy the matrices can be safely truncated with an error that is given by Eq. 2.6; the maximal size of the matrices is called the bond dimension D. We can now represent this *matrix product state* pictorially as

$|\Psi\rangle =$ 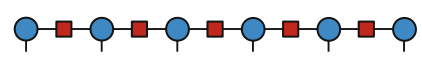 ,

where every blue circle represents a Γ tensor – the index i is represented as the middle "physical" leg – and every red square is a Λ matrix.

Another way of arriving at a matrix product state is in the spirit of the AKLT construction above. In a so-called valence bond solid [216] two ancilla degrees of freedom $|\alpha\rangle_{a,i}$ and $|\alpha\rangle_{b,i}$ are attached to every physical site i, and ancillas from neighbouring sites are brought into a maximally entangled state

$$|\phi\rangle_{i,i+1} = \sum_{\gamma} |\gamma\rangle_{b,i} \otimes |\gamma\rangle_{a,i+1}.$$

A physical state $|\Psi\rangle$ is obtained by projecting the two ancillas onto a physical spin at every site i with the projection operator

$$P_i = \sum_{s=1}^{d} \sum_{\alpha,\beta} A^{[i],s}_{\alpha,\beta} |s\rangle \left(\langle\alpha|_{a,i} \otimes \langle\beta|_{b,i} \right).$$

If the system has open boundary conditions, two ancillas remain unpaired. The advantage of this construction, however, is that the case of periodic boundary conditions is easily considered by placing these two unpaired ancillas in an entangled state as well [217]. The state that is obtained in this way is given by

$$\begin{aligned} |\Psi\rangle &= \sum_{i_1,\ldots,i_N} \sum_{\gamma_1,\ldots,\gamma_N} A^{[1],i_1}_{\gamma_N,\gamma_1} A^{[2],i_2}_{\gamma_1,\gamma_2} \cdots A^{[N-1],i_{N-1}}_{\gamma_{N-2},\gamma_{N-1}} A^{[N],i_N}_{\gamma_{N-1},\gamma_N} |i_1,\ldots,i_N\rangle \\ &= \sum_{i_1,\ldots,i_N} \mathrm{Tr}\left(A^{[1],i_1} A^{[2],i_2} \cdots A^{[N-1],i_{N-1}} A^{[N],i_N} \right) |i_1,\ldots,i_N\rangle \end{aligned}$$

where in the second line we have again introduced a matrix-product notation. Note that the projection transforms a product state of valence bonds into a state with finite-range entanglement. In fact, this form is equivalent to the state in Eq. 2.7 up to the boundary conditions, so that we have again obtained an MPS, now represented as

$|\Psi\rangle =$ 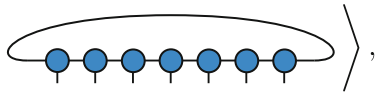 ,

with every blue circle an MPS tensor A, again with the physical index i in the middle.

A third interpretation of the class of MPS is in terms of the holographic principle. An MPS can be thought of as being generated by a D-level auxiliary system that interacts sequentially with the different spins on the lattice [218–220]. The spatial correlations of the state that is generated is directly related to the temporal correlations of the auxiliary system. This shows that an MPS can be described by the dissipative dynamics of a lower-dimensional auxiliary system, providing a holographic interpretation that can be extended to higher-dimensional settings as well.

Properties of MPS

The viability of MPS as a variational class was clear from the outset because of the success of DMRG, but it proved that investigating the properties of MPS in a more formal fashion would open up a whole new range of applications.

For our purposes, it suffices to consider the set of translation-invariant MPS on a chain of N sites with periodic boundary conditions

$$|\Psi(A)\rangle = \sum_{i_1,\ldots,i_N} \mathrm{Tr}\left(A^{i_1}A^{i_2}\cdots A^{i_N}\right)|i_1,\ldots,i_N\rangle. \tag{2.8}$$

In this form, the same $D \times d \times D$ tensor A is repeated on every site, so it is translation invariant by construction; it can be shown that every translation-invariant MPS can be brought into this form [221]. Closely connected to this MPS is the completely positive map $\mathcal{E}$ acting on the space of $D \times D$ matrices as

$$\mathcal{E}(X) = \sum_i A^i X (A^i)^\dagger.$$

In the generic[14] case [221] this map has a leading eigenvalue equal to one, and all other eigenvalues within the unit circle. The leading eigenvector or fixed point of $\mathcal{E}$ is guaranteed [222] to be a positive matrix Λ.

Now it is clear that there is a redundancy in the parametrization of the state $|\Psi(A)\rangle$ in terms of the tensor A because the gauge transformation

$$A^i \to X^{-1}A^i X \qquad \forall i$$

leaves the state invariant. This gauge freedom leaves the possibility to define a normal or canonical form [221] for the tensor A by imposing that the fixed point of the cp map is the unit matrix, i.e.

$$\sum_i A^i (A^i)^\dagger = \mathbb{1}.$$

Now the fundamental theorem of MPS states that this canonical form is unique up to an additional unitary gauge transformation for any generic MPS [221, 223]. This implies that if two MPS $|\Psi(A_1)\rangle$ and $|\Psi(A_2)\rangle$ are equal there should exist a gauge transform that links the two MPS tensors A_1 and A_2.

From the form in Eq. (2.7) it is clear that the bipartite entanglement entropy of an MPS is bounded by $\log D$ and, if the bond dimension is kept finite, obeys the area law of entanglement entropy. Therefore, it seems plausible that an MPS can

[14] The generic case excludes the cases where the MPS can be written as (i) the superposition of multiple translation-invariant MPSs with smaller bond dimension or (ii) the superposition of p p-periodic states each of which can be written as an MPS. The condition under which an MPS is generic is related to the injectivity of the MPS, which means that by concatenating enough A tensors the map from the virtual space to the physical one becomes injective, and to the fact that there is only eigenvalue of $\mathcal{E}$ on the unit circle [221].

approximate any state with an area law, such as ground states of local Hamiltonians [58, 224]. This statement was made rigorous in Ref. [56] where it was indeed proven that ground states of local gapped Hamiltonians can be approximated by MPS. This implies that the class of matrix product states provides a dense parametrization of all gapped phases in one dimension. For ground states of critical Hamiltonians, for which the entanglement entropy of a block scales logarithmically with the size, an MPS approximation needs a bond dimension that scales polynomially in the system size [225].

This description of all gapped ground states in one dimension can be lifted to the level of Hamiltonians. As we have seen, matrix product states are generalizations of the valence bond solids, which were proven to be the unique ground states of local Hamiltonians. It appears that this property is general: any MPS is the unique ground state of a local gapped Hamiltonian, called the parent Hamiltonian [221]. Since we know that the ground state of a given Hamiltonian can be well approximated by an MPS, this allows to replace this original Hamiltonian by the parent Hamiltonian of the MPS. This replacing can be done without closing the gap, so that we can represent all gapped Hamiltonians within a certain phase by a well-chosen parent Hamiltonian. In this way, the classification of all gapped quantum phases can be done by tracing paths of MPS and their parent Hamiltonians. If one imposes that certain physical symmetries have to be preserved on these paths – these physical symmetries are reflected in the MPS language as projective representations on the MPS's virtual degrees of freedom [226] – it appears that there are so-called symmetry-protected topological phases that do not connect to a trivial phase without breaking these symmetries [227–229].

Implicit in all these considerations is the assumption that the number of sites N should be large, such that the MPS describes the bulk physics of a spin chain. In the original DMRG algorithm numerical resources scale linearly in the system size, but it is clear that for the translation-invariant form of Eq. (2.8) the limit to infinitely large systems can easily be taken [213, 230–232].

2.6.4 Simulating Spin Chains with MPS

The success of MPS for simulating spin chains is mostly based on the fact that expectation values and correlation functions of an MPS can be computed in an efficient way.[15] Importantly, an MPS always has exponential decay of correlations, which shows again that they are not the right variational class to simulate critical models. In this section, we review the different MPS algorithms for computing the properties of spin chains.

[15] We refer to the reviews [189, 191, 202] for a detailed account.

Approximating Ground States

We have seen that the ground state of every (gapped) local Hamiltonian H can be represented as an MPS $|\Psi(\{A_i\})\rangle$, but the challenge remains of finding this optimal state efficiently within the MPS manifold. According to the variational principle, this problem of optimizing the variational parameters $\{A_i\}$ can be written as a minimization problem for the energy functional,

$$\min_{\{A_i\}} \frac{\langle\Psi(\{A_i\})|H|\Psi(\{A_i\})\rangle}{\langle\Psi(\{A_i\})|\Psi(\{A_i\})\rangle}.$$

Finding the optimal set of tensors $\{A_i\}$ is a highly non-linear optimization problem, and is infeasible to solve in one stretch. Luckily, there is a way out of this by realizing that the energy functional is quadratic for every tensor A_i separately, so that the optimization for one tensor can be easily solved by a generalized eigenvalue problem. An efficient algorithm is then obtained by sweeping back and forth through the chain and optimizing every tensor separately at each iteration. Moreover, by fixing the gauge of the MPS tensors in a smart way, the normalization for each tensor can be made trivial, such that the on-site optimization reduces to an ordinary eigenvalue problem. This algorithm is variational in the sense that the energy is lowered at every step in the algorithm. In fact, it appears that this algorithm is almost identical to the one-site version of DMRG [202, 233], a connection that also explains the success of standard DMRG implementations.

For translation-invariant MPS in the thermodynamic limit, where the MPS $|\Psi(A)\rangle$ is parametrized by one single tensor A, this DMRG procedure obviously no longer works. There are essentially three different methods for optimizing infinite MPS:

- Infinite DMRG. This algorithm is a translation of the original infinite-system DMRG [198, 199] into the MPS language. The central idea is the growing of the system by iteratively inserting new sites in the middle and variationally optimizing the MPS tensors on the newly inserted sites. This procedure is repeated until the state has converged in the middle to some description of the bulk physics of the system. The MPS reformulation has led to a tremendous improvement on the original DMRG algorithm through a so-called state prediction, which provides an initial guess for the optimization of the inserted tensors based on the previous iteration [234], see also [235].
- Infinite time-evolving block decimation. This method finds the ground state by evolving a well-chosen initial state with the imaginary-time evolution operator $\mathrm{e}^{-H\tau}$; in the limit $\tau \to \infty$ this results in a projection on the ground state. The time evolution is implemented with a Trotter–Suzuki decomposition and, after each time step, truncating the MPS to a certain bond dimension [230]. This truncation is done by considering the truncation of one bond in the MPS and substituting these locally optimal MPS tensors throughout the infinite chain – a procedure that is not guaranteed to be optimal. Because imaginary-time evolution is non-unitary, the MPS should in principle be orthonormalized in every iteration [231].

- Tangent-space methods. In this set of methods the manifold structure of the variational class of MPS is taken seriously, and implementations typically reduce to operations with vectors in the tangent space on the manifold [236]. In particular, imaginary time-evolution is performed in the MPS manifold by projecting the time evolution onto the tangent space, according to the time-dependent variational principle [232]. Alternatively, one could implement a conjugate-gradient optimization within the MPS manifold, where, in every iteration of the optimization, the gradient of the energy functional is a vector in the tangent space [237]; more advanced optimization strategies can take into account the non-trivial geometry of the MPS manifold [238]. Tangent-space methods have the advantage of relying on globally optimal routines only, but often at a higher numerical cost.

Dynamical Properties

Ground-state algorithms can be straightforwardly extended to also capture excited states. In the case where the ground state and the first excitations of a system live in different sectors characterized by different quantum numbers, then an energy minimization in the right sector will lead to these excited states. If the sectors are the same, the excitations have to be computed iteratively, where one particular excitation is targeted by, throughout the algorithm, orthonormalizing with respect to all lower-lying states that were found in a previous run. This implies that a simple adaptation of the DMRG algorithm allows to compute e.g. the gap of generic spin chains.

Typically, however, real interest lies in capturing excitations with well-defined momentum such that dispersion relations can be computed. Therefore, systems with periodic boundary conditions should be treated, which are a lot harder to simulate with DMRG [217, 239], especially if a translation-invariant ground state is wanted [240]. Although the targeting of excitations within a particular momentum sector has been implemented in Ref. [241], the scope of dynamical DMRG simulations has shifted to other approaches.

One of the main interests is the simulation of quantum quenches, i.e. the time evolution of a system after a sudden change of a parameter in the Hamiltonian. All standard approaches for simulating real-time evolution rely on the Trotter–Suzuki decomposition of the evolution operator e^{-iHt}, often in the form of a matrix product operator [242], and subsequent truncations of the bond dimension [202, 214, 215, 243–245]. Other approaches are based on the time-dependent variational principle [232, 246]. The time evolution after a local perturbation on a translation-invariant background can be simulated by introducing a finite window that is grown as time increases [247–249].

Equally important is the dynamical spin structure factor or spectral function

$$S(q,\omega) = \sum_n \mathrm{e}^{-iqn} \int_{-\infty}^{+\infty} \mathrm{e}^{i\omega t}\ \langle 0|S_n^\alpha(t) S_0^\alpha(0)|0\rangle,$$

and different schemes have been developed within the DMRG framework for its evaluation:

- Lanczos algorithms. The first attempt was made by Hallberg [250] by using a continued-fraction expansion based on a Lanczos algorithm. The central idea in this approach is the construction of a number of Lanczos vectors by a multitarget DMRG, where the DMRG basis is optimized for the ground state and Lanczos states simultaneously. This method was improved recently [251] by calculating the Lanczos vectors adaptively, i.e., only the three last states are kept in the recursion. This method was recently much improved by implementing it in the MPS/MPO language [252].
- Correction vector method. The spectral function at a certain energy can be computed as the spectral weight of a so-called correction vector, which can be computed with conventional DMRG methods [253–255] or variational MPS methods [256]. This method is quite expensive as this correction vector has to be computed for every ω separately, involving an operator inversion problem.
- Real-time evolution. The time-domain correlator can be computed using real-time evolution algorithms, so that a Fourier transform gives direct access to the spectral function. The time-dependence can be further interpolated using linear prediction techniques [257–261]. This method is limited by the growth of entanglement during real-time evolution.
- Chebyshev expansion. Spectral functions can be represented approximately by a Chebyshev expansion, which can be computed efficiently with MPS methods [262].

Although these methods differ a lot in implementation and efficiency, they share the same basic strategy: one starts from the action of a local operator on the ground state and captures different operations on this state within the space of MPS. The action of this local operator, however, generates not only the low-lying physics that one is interested in, but also excites higher-energy eigenstates of the system. These higher-energy modes are only eliminated at a final stage, when one looks only at the low-energy part of the spectral function.

From the perspective that we take in this dissertation, this is a clear disadvantage: it is a lot more natural to search for an efficient parametrization of the low-energy subspace first, such that the action of the local operator can be projected on this low-energy space from the start. This approach has the additional advantage that one can target non-extensive properties on a ground state in the thermodynamic limit, which is impossible if one stays within the original space of matrix product states. Instead, we will show in this dissertation that the low-lying dynamics above an MPS ground state are captured within the tangent space, rather than the original manifold itself – see Sect. 3.5.

Finally, it should be noted that also finite-temperature simulations have come within the reach of MPS methods [245, 263, 264], which led to algorithms for computing spectral properties [259] and real-time evolution [265].

2.6.5 *Projected Entangled-Pair States*

In principle any quantum state can be decomposed as a matrix product state, irrespective of the dimensionality or geometry of the lattice on which it is defined – as long as the bond dimension is chosen large enough. This implies that DMRG and other MPS methods can also be applied to e.g. two-dimensional quantum spin systems. Yet, despite some success [98, 266, 267], it should be obvious that the class of MPS is not a correct variational state for capturing ground states of two-dimensional systems, because MPS do not have the correct entanglement structure for describing a two-dimensional ground state.

A more natural choice is the class of projected entangled-pair states (PEPS), which are easily obtained by generalizing the valence-bond construction to two- and higher-dimensional geometries [216, 268]. For the two-dimensional square lattice, we put four ancilla degrees of freedom on every physical site, put neighbouring ancillas into maximally entangled states and project them onto the physical spins. A PEPS is thus represented as

$$|\Psi\rangle = \sum_{i_{11},i_{12},\ldots} C_2(A^{i_{11}} A^{i_{12}} \cdots)|i_{11}, i_{12}, \ldots\rangle$$

where a part of the contraction can be represented as

$C_2(A^{i_{11}} A^{i_{12}} \cdots) =$

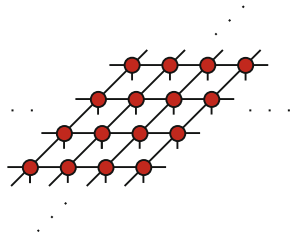

In this definition, A is now a 5-legged tensor with four virtual legs, carrying the quantum correlations in the state, and one physical leg corresponding to the physical spins of the system.

From the above form it is clear that a PEPS has a built-in area law for the entanglement entropy, a property that is shared by many ground states of local Hamiltonians. In contrast to the one-dimensional case, this cannot be rigorously proven in the higher-dimensional setting. Still, every PEPS has a parent Hamiltonian and, if the PEPS is injective, it is the unique ground state [270]. There a few interesting two-dimensional quantum states that have an exact PEPS representation, viz. the two-dimensional AKLT states [79, 80], resonating valence-bond states [97, 269, 271], the toric-code state [116, 269], and, more generally, string nets [272, 273].

Interestingly, whereas MPS could only exhibit exponential decay of correlations, a PEPS can also contain power-law decay of correlations [269]. The way to construct a "critical" PEPS is by noting that to every system of statistical mechanics a quantum state can be associated for which the expectation values of quantum observables reduce to the classical expectation values. If the classical system is now tuned to a critical point – the easiest example is the two-dimensional Ising model [269] – the corresponding PEPS has critical correlations. It seems, however, that the correlations in this state have a classical origin, and, consequently, this property does not imply that two-dimensional quantum critical systems can be captured accurately with PEPS. Another crucial difference is that the norm or expectation values of PEPS cannot be computed efficiently in principle; the cost of contracting the two-dimensional network corresponding to the norm of a PEPS scales exponentially in the number of sites of the lattice [274]. In practice, numerical algorithms still allow to do this efficiently by representing subregions of the lattice as tensor networks. This allows to determine effective environments for local regions in the PEPS such that local expectation values can be evaluated. In Chap. 5 we will review the different algorithms in more detail.

Despite the progress in numerical algorithms, the contraction of a PEPS is still a computationally demanding task, which makes PEPS simulations a rather tedious endeavour. The challenge of finding an optimal PEPS representation for the ground state of a two-dimensional quantum spin system is, in absence of a two-dimensional analogue of DMRG, still in the stage of finding efficient algorithms. All state-of-the-art methods are based on imaginary-time evolution with two-dimensional versions of the time-evolving block decimation, a method that is non-variational and, as such, not completely under control as it is not guaranteed to reach a variational minimum. In Chap. 5 we will consider these different algorithms and present our own variational method for optimizing the PEPS representation of generic ground states.

Next to the viability of PEPS as a variational ansatz for approximating a ground state of a two-dimensional quantum system, they also offer interesting theoretical insights into the entanglement structure of two-dimensional quantum systems. Firstly, they capture bulk-boundary correspondences in a natural way; the unpaired virtual degrees of freedom that appear as a PEPS is cut in half, can be identified with the entanglement spectrum of the subregions, allowing to determine boundary Hamiltonians in a natural way [275, 276]; in addition, one can follow the effect of perturbations in the bulk on the edge physics [277]. Secondly, PEPS allow to consider topologically ordered states in a natural way. Indeed, it was observed that topological order of a PEPS is manifested as a symmetry on the virtual level of the PEPS tensors and that the non-trivial properties of the anyonic excitations can be understood from strings living on the virtual level of the PEPS [278–281]. Also, topological phase transitions can be modelled by perturbing these PEPS in a specific way [276, 282, 283]. It still remains a big question, however, to what extent PEPS can classify all two-dimensional quantum phases.

2.6.6 *Significant Other*

Both MPS and PEPS succeed in capturing the physics of low-energy states of local Hamiltonians by modeling their entanglement structure in the form of a tensor network. In recent years, this fundamental idea has been extended to other quantum many-body states with different entanglement properties. Neglecting any attempt at being exhaustive, let us highlight two other types of tensor networks.

Firstly, we have repeatedly mentioned that MPS fail to capture the properties of critical spin chains, because of the logarithmic scaling of the entanglement entropy and the algebraic decay of correlations. Therefore, in order to capture the ground state of critical spin chain models, the multi-scale entanglement renormalization ansatz has been introduced [284]. In this ansatz, the idea of renormalization group transformations is explicitly modelled, such that, in contrast to the case of MPS [285], it is tailored to sustain a renormalization flow along a newly introduced scale dimension of the network. As such, it can give rise to scale-invariant states at criticality, with the correct entanglement and correlation properties. The same idea has been applied to impurity problems [286], making the connection with the numerical renormalization group of Wilson, and has led to a better understanding of the transfer matrix of an MPS [287, 288].

Secondly, the idea of MPS can be extended to the description of ground states of one-dimensional quantum field theories, by taking the appropriate continuum limit [220, 289–291]. These continuous matrix product states have been successfully applied to capture the ground state, excitations, and real-time dynamics of Bose gases [292–294] and has led to a non-commutative version of the Gross–Pitaevskii equation [295].

2.7 Renormalization and Effective Particles

One concept that we haven't really touched upon is the renormalization group [192, 296], which embraces a set of ideas and procedures that are designed to eliminate irrelevant degrees of freedom in order to arrive at a low-energy effective description for a many-body system. Both in high-energy particle physics [297] and condensed-matter physics [14, 298], such an effective description is typically given in terms of a quantum field theory; for the latter, the fields describe the long-wavelength fluctuations that occur in a quantum material.

One such effective-field construction is Fermi-liquid theory [299, 300], describing the low-energy behaviour of a system of interacting fermions in terms of effective quasiparticles [301, 302]. These quasiparticles are defined starting from the free electrons in the non-interacting limit, and, by adiabatically turning on the interactions, the electrons gain renormalized masses, charges and lifetimes. Close to the Fermi surface, the quasiparticle lifetime diverges and the dressed electrons remain well-defined modes of the system, so that their dynamics explain the low-energy behaviour of a Fermi-liquid.

This idea of capturing the low-energy physics of quantum many-body systems in terms of effective particle-like degrees of freedom is all-around in condensed-matter physics. In the field of strongly-correlated quantum matter, however, they are not defined starting from a non-interacting limit, but they appear as collective modes on top of a strongly-correlated ground state. The long-ranged quantum correlations (entanglement) in the ground state allow for these particles to have exotic emergent properties such as fractional quantum numbers and non-conventional statistics [see Sect. 2.3]. They come under the names of phonons, magnons, spinons, holons, solitons, visons, anyons, etc.

In the following chapters effective particles will play a central role. The way we will arrive at them, however, will be quite different, without field-theory methods such as functional integration. Instead, we will start from the ground state of a microscopic Hamiltonian, on which we build the elementary excitations variationally. Only in a next step we will interpret the excitations as "particles" and start building an effective theory.

References

1. P.A.M. Dirac, Quantum mechanics of many-electron systems. Proc. R. Soc. Lond. Ser. A **123**, 714 (1929). doi:10.1098/rspa.1929.0094
2. E. Schrödinger, Discussion of probability relations between separated systems. Math. Proc. Camb. Philos. Soc. **31**, 555 (1935). doi:10.1017/S0305004100013554
3. A. Einstein, B. Podolsky, N. Rosen, Can quantum-mechanical description of physical reality be considered complete? Phys. Rev. **47**, 777 (1935). doi:10.1103/PhysRev.47.777
4. P.A.M. Dirac, Note on exchange phenomena in the Thomas atom. Math. Proc. Camb. Philos. Soc. **26**, 376 (1930). doi:10.1017/S0305004100016108
5. J. von Neumann, *Mathematische Grundlagen der Quantenmechanik* (Springer, Berlin, 1932)
6. J.J. Sakurai, *Modern Quantum Mechanics* (The Benjamin/Cummings Publishing Company Inc, San Francisco, 1985)
7. J. Hubbard, Electron correlations in narrow energy bands. Proc. R. Soc. A Math. Phys. Eng. Sci. **276**, 238 (1963). doi:10.1098/rspa.1963.0204
8. F.H.L. Essler, H. Frahm, F. Göhmann, A. Klümper, V.E. Korepin, *The One-Dimensional Hubbard Model* (Cambridge University Press, Cambridge, 2005)
9. A. Auerbach, *Interacting Electrons and Quantum Magnetism* (Springer, Berlin, 1994)
10. A. Altland, B. Simons, *Condensed Matter Field Theory* (Cambridge University Press, Cambridge, 2006)
11. W. Heisenberg, Zur Theorie des Ferromagnetismus. Zeitschrift für Physik **49**, 619 (1928). doi:10.1007/BF01328601
12. P.W. Anderson, Antiferromagnetism. theory of superexchange interaction. Phys. Rev. **79**, 350 (1950). doi:10.1103/PhysRev.79.350
13. A.L. Fetter, J.D. Walecka, *Quantum Theory of Many-Particle Systems* (McGraw-Hill, San Francisco, 1971)
14. A.M. Tsvelik, *Quantum Field Theory in Condensed Matter Physics* (Cambridge University Press, Cambridge, 1995)
15. S. Sachdev, *Quantum Phase Transitions* (Cambridge University Press, Cambridge, 2011)
16. L. Landau, On the theory of phase transitions. Zh. Eksp. Teor. Fiz. **7**, 19 (1937)
17. P. Pfeuty, The one-dimensional Ising model with a transverse field. Ann. Phys. **57**, 79 (1970). doi:10.1016/0003-4916(70)90270-8

18. N.F. Mott, The basis of the electron theory of metals, with special reference to the transition metals. Proc. Phys. Soc. Sect. A **62**, 416 (1949). doi:10.1088/0370-1298/62/7/303
19. M. Imada, A. Fujimori, Y. Tokura, Metal-insulator transitions. Rev. Mod. Phys. **70**, 1039 (1998). doi:10.1103/RevModPhys.70.1039
20. J.G. Bednorz, K.A. Müller, Possible high T_c superconductivity in the Ba-La-Cu-O system. Zeitschrift für Physik B Condensed Matter **64**, 189 (1986). doi:10.1007/BF01303701
21. C. Broholm, G. Aeppli, Dynamic correlations in quantum magnets, *Strong Interactions in Low Dimensions* (Springer, Netherlands, 2004), pp. 21–61. doi:10.1007/978-1-4020-3463-3_2
22. S.T. Bramwell, Neutron scattering in highly frustrated magnetism, in *Introduction to Frustrated Magnetism*, ed. by C. Lacroix, F. Mila, P. Mendels (Springer, Berlin, 2011), pp. 45–78. doi:10.1007/978-3-642-10589-0
23. C. Lacroix, P. Mendels, F. Mila, *Introduction to Frustrated Magnetism* (Springer, Berlin, 2011)
24. M.H. Anderson, J.R. Ensher, M.R. Matthews, C.E. Wieman, E.A. Cornell, Observation of Bose-Einstein Condensation in a dilute atomic vapor. Science **269**, 198 (1995). doi:10.1126/science.269.5221.198
25. K.B. Davis, M.O. Mewes, M.R. Andrews, N.J. van Druten, D.S. Durfee, D.M. Kurn, W. Ketterle, Bose-Einstein condensation in a gas of sodium atoms. Phys. Rev. Lett. **75**, 3969 (1995). doi:10.1103/PhysRevLett.75.3969
26. I. Bloch, Ultracold quantum gases in optical lattices. Nat. Phys. **1**, 23 (2005). doi:10.1038/nphys138
27. I. Bloch, W. Zwerger, Many-body physics with ultracold gases. Rev. Mod. Phys. **80**, 885 (2008). doi:10.1103/RevModPhys.80.885
28. I. Bloch, J. Dalibard, S. Nascimbène, Quantum simulations with ultracold quantum gases. Nat. Phys. **8**, 267 (2012). doi:10.1038/nphys2259
29. M.P.A. Fisher, P.B. Weichman, G. Grinstein, D.S. Fisher, Boson localization and the superfluid-insulator transition. Phys. Rev. B **40**, 546 (1989). doi:10.1103/PhysRevB.40.546
30. D. Jaksch, C. Bruder, J.I. Cirac, C. Gardiner, P. Zoller, Cold bosonic atoms in optical lattices. Phys. Rev. Lett. **81**, 3108 (1998). doi:10.1103/PhysRevLett.81.3108
31. M. Greiner, O. Mandel, T. Esslinger, T.W. Hänsch, I. Bloch, Quantum phase transition from a superfluid to a Mott insulator in a gas of ultracold atoms. Nature **415**, 39 (2002). doi:10.1038/415039a
32. B. Paredes, A. Widera, V. Murg, O. Mandel, S. Folling, J.I. Cirac, G.V. Shlyapnikov, T.W. Hänsch, I. Bloch, Tonks–Girardeau gas of ultracold atoms in an optical lattice. Nature **429**, 277 (2004), http://www.nature.com/nature/journal/v429/n6989/suppinfo/nature02530_S1.html
33. T. Kinoshita, T. Wenger, D.S. Weiss, Observation of a one-dimensional Tonks-Girardeau gas. Science **305**, 1125 (2004). doi:10.1126/science.1100700
34. T. Kinoshita, T. Wenger, D.S. Weiss, A quantum Newton's cradle. Nature **440**, 900 (2006), http://www.nature.com/nature/journal/v440/n7086/suppinfo/nature04693_S1.html
35. J. Simon, W.S. Bakr, R. Ma, M.E. Tai, P.M. Preiss, M. Greiner, Quantum simulation of antiferromagnetic spin chains in an optical lattice. Nature **472**, 307 (2011). doi:10.1038/nature09994
36. J. Struck, C. Olschlager, R. Le Targat, P. Soltan-Panahi, A. Eckardt, M. Lewenstein, P. Windpassinger, K. Sengstock, Quantum simulation of frustrated classical magnetism in triangular optical lattices. Science **333**, 996 (2011). doi:10.1126/science.1207239
37. R. Blatt, C.F. Roos, Quantum simulations with trapped ions. Nat. Phys. **8**, 277 (2012). doi:10.1038/nphys2252
38. D. Porras, J.I. Cirac, Effective quantum spin systems with trapped ions. Phys. Rev. Lett. **92**, 207901 (2004). doi:10.1103/PhysRevLett.92.207901
39. A. Aspuru-Guzik, P. Walther, Photonic quantum simulators. Nat. Phys. **8**, 285 (2012). doi:10.1038/nphys2253
40. X.-S. Ma, B. Dakic, W. Naylor, A. Zeilinger, P. Walther, Quantum simulation of the wavefunction to probe frustrated Heisenberg spin systems. Nat. Phys. **7**, 399 (2011). doi:10.1038/nphys1919

41. J.I. Cirac, P. Zoller, Goals and opportunities in quantum simulation. Nat. Phys. **8**, 264 (2012). doi:10.1038/nphys2275
42. I. Buluta, F. Nori, Quantum simulators. Science **326**, 108 (2009). doi:10.1126/science.1177838
43. R.P. Feynman, Simulating physics with computers. Int. J. Theor. Phys. (1982), http://www.springerlink.com/index/T2X8115127841630.pdf
44. M.A. Nielsen, I.L. Chuang, *Quantum Computation and Quantum Information* (Cambridge University Press, Cambridge, 2000)
45. T.J. Osborne, M.A. Nielsen, Entanglement, quantum phase transitions, and density matrix renormalization. Quantum Inf. Process. **1**, 45 (2002). doi:10.1023/A:1019601218492
46. G. Vidal, J.I. Latorre, E. Rico, A. Kitaev, Entanglement in quantum critical phenomena. Phys. Rev. Lett. **90**, 227902 (2003). doi:10.1103/PhysRevLett.90.227902
47. A. Kitaev, J. Preskill, Topological entanglement entropy. Phys. Rev. Lett. **96**, 110404 (2006). doi:10.1103/PhysRevLett.96.110404
48. M. Levin, X.-G. Wen, Detecting topological order in a ground state wave function. Phys. Rev. Lett. **96**, 110405 (2006). doi:10.1103/PhysRevLett.96.110405
49. X. Chen, Z.-C. Gu, X.-G. Wen, Local unitary transformation, long-range quantum entanglement, wave function renormalization, and topological order. Phys. Rev. B **82**, 155138 (2010). doi:10.1103/PhysRevB.82.155138
50. J. Preskill, Quantum Information and Computation (Lecture Notes) (2016), http://www.theory.caltech.edu/people/preskill/ph229/
51. J. Preskill, Quantum information and physics: some future directions. J. Mod. Opt. **47**, 127 (2000). doi:10.1080/09500340008244031
52. M.B. Hastings, Locality in Quantum Systems (2010), arXiv:1008.5137
53. J. Eisert, M. Cramer, M.B. Plenio, Colloquium: area laws for the entanglement entropy. Rev. Mod. Phys. **82**, 277 (2010). doi:10.1103/RevModPhys.82.277
54. E.H. Lieb, D.W. Robinson, The finite group velocity of quantum spin systems. Commun. Math. Phys. **28**, 251 (1972). doi:10.1007/BF01645779
55. M.B. Hastings, T. Koma, Spectral gap and exponential decay of correlations. Commun. Math. Phys. **265**, 781 (2006). doi:10.1007/s00220-006-0030-4
56. M.B. Hastings, An area law for one-dimensional quantum systems. J. Stat. Mech. Theory Exp. **2007**, P08024 (2007). doi:10.1088/1742-5468/2007/08/P08024
57. P. Calabrese, J. Cardy, Entanglement entropy and quantum field theory. J. Stat. Mech. Theory Exp. **2004**, P06002 (2004). doi:10.1088/1742-5468/2004/06/P06002
58. F. Verstraete, J.I. Cirac, Matrix product states represent ground states faithfully. Phys. Rev. B **73**, 094423 (2006). doi:10.1103/PhysRevB.73.094423
59. Z. Landau, U. Vazirani, T. Vidick, A polynomial-time algorithm for the ground state of 1D gapped local Hamiltonians (2013), arXiv:1307.5143
60. V. Coffman, J. Kundu, W.K. Wootters, Distributed entanglement. Phys. Rev. A **61**, 052306 (2000). doi:10.1103/PhysRevA.61.052306
61. T.J. Osborne, F. Verstraete, General monogamy inequality for bipartite qubit entanglement. Phys. Rev. Lett. **96**, 220503 (2006). doi:10.1103/PhysRevLett.96.220503
62. N.D. Mermin, H. Wagner, Absence of ferromagnetism or antiferromagnetism in one- or two-dimensional isotropic Heisenberg models. Phys. Rev. Lett. **17**, 1133 (1966). doi:10.1103/PhysRevLett.17.1133
63. P.C. Hohenberg, Existence of long-range order in one and two dimensions. Phys. Rev. **158**, 383 (1967). doi:10.1103/PhysRev.158.383
64. S. Coleman, There are no Goldstone bosons in two dimensions. Commun. Math. Phys. **31**, 259 (1973). doi:10.1007/bf01646487
65. P.W. Anderson, An approximate quantum theory of the antiferromagnetic ground state. Phys. Rev. **86**, 694 (1952). doi:10.1103/PhysRev.86.694
66. S. Chakravarty, B.I. Halperin, D.R. Nelson, Two-dimensional quantum Heisenberg antiferromagnet at low temperatures. Phys. Rev. B **39**, 2344 (1989). doi:10.1103/PhysRevB.39.2344

67. H. Bethe, Zur Theorie der Metalle. I. Eigenwerte und Eigenfunktionen der linearen Atomkette. Zeitschrift für Physik **71**, 205 (1931). doi:10.1007/BF01341708
68. L. Hulthén, Über das Austauschproblem eines Kristalles. Arkiv för matematik, astronomi och fysik **26A**, 11 (1938)
69. R. Kubo, The spin-wave theory of antiferromagnetics. Phys. Rev. **87**, 568 (1952). doi:10.1103/PhysRev.87.568
70. T. Oguchi, Theory of spin-wave interactions in ferro- and antiferromagnetism. Phys. Rev. **117**, 117 (1960). doi:10.1103/PhysRev.117.117
71. T. Holstein, H. Primakoff, Field dependence of the intrinsic domain magnetization of a ferromagnet. Phys. Rev. **58**, 1098 (1940). doi:10.1103/PhysRev.58.1098
72. F.J. Dyson, General theory of spin-wave interactions. Phys. Rev. **102**, 1217 (1956). doi:10.1103/PhysRev.102.1217
73. T. Giamarchi, *Quantum Physics in One Dimension* (Oxford University Press, Oxford, 2004)
74. E.H. Lieb, T. Schultz, D. Mattis, Two soluble models of an antiferromagnetic chain. Ann. Phys. **16**, 407 (1961). doi:10.1016/0003-4916(61)90115-4
75. I. Affleck, E.H. Lieb, A proof of part of Haldane's conjecture on spin chains. Lett. Math. Phys. **12**, 57 (1986). doi:10.1007/BF00400304
76. F.D.M. Haldane, Continuum dynamics of the 1-D Heisenberg antiferromagnet: identification with the O(3) nonlinear sigma model. Phys. Lett. A **93**, 464 (1983). doi:10.1016/0375-9601(83)90631-X
77. F.D.M. Haldane, Nonlinear field theory of large-spin Heisenberg antiferromagnets: semiclassically quantized solitons of the one-dimensional easy-axis nNeel state. Phys. Rev. Lett. **50**, 1153 (1983). doi:10.1103/PhysRevLett.50.1153
78. I. Affleck, Quantum spin chains and the Haldane gap. J. Phys. Condens. Matter **1**, 3047 (1989), http://cat.inist.fr/?aModele=afficheN&cpsidt=6916826
79. I. Affleck, T. Kennedy, E.H. Lieb, H. Tasaki, Rigorous results on valence-bond ground states in antiferromagnets. Phys. Rev. Lett. **59**, 799 (1987). doi:10.1103/PhysRevLett.59.799
80. I. Affleck, T. Kennedy, E.H. Lieb, H. Tasaki, Valence bond ground states in isotropic quantum antiferromagnets. Commun. Math. Phys. **115**, 477 (1988). doi:10.1007/BF01218021
81. M. Nightingale, H. Blöte, Gap of the linear spin-1 Heisenberg antiferromagnet: a Monte Carlo calculation. Phys. Rev. B **33**, 659 (1986). doi:10.1103/PhysRevB.33.659
82. F.D.M. Haldane, Errata. Phys. Lett. A **81**, 545 (1981). doi:10.1016/0375-9601(81)90464-3
83. A. Imambekov, T.L. Schmidt, L.I. Glazman, One-dimensional quantum liquids: beyond the Luttinger liquid paradigm. Rev. Mod. Phys. **84**, 1253 (2012). doi:10.1103/RevModPhys.84.1253
84. F.D.M. Haldane, Effective harmonic-fluid approach to low-energy properties of one-dimensional quantum fluids. Phys. Rev. Lett. **47**, 1840 (1981). doi:10.1103/PhysRevLett.47.1840
85. F.D.M. Haldane, Demonstration of the Luttinger liquid character of Bethe-ansatz-soluble models of 1-D quantum fluids. Phys. Lett. **81**, 153 (1981), http://www.sciencedirect.com/science/article/pii/0375960181900499
86. F.D.M. Haldane, General relation of correlation exponents and spectral properties of one-dimensional fermi systems: application to the anisotropic S = 1/2 Heisenberg chain. Phys. Rev. Lett. **45**, 1358 (1980). doi:10.1103/PhysRevLett.45.1358
87. S.-I. Tomonaga, Remarks on Bloch's method of sound waves applied to many-fermion problems. Prog. Theor. Phys. **5**, 544 (1950). doi:10.1143/ptp/5.4.544
88. J.M. Luttinger, An exactly soluble model of a many-fermion system. J. Math. Phys. **4**, 1154 (1963). doi:10.1063/1.1704046
89. J. Cardy, *Scaling and Renormalization in Statistical Physics* (Cambridge University Press, Cambridge, 1996)
90. L.D. Faddeev, L.A. Takhtajan, What is the spin of a spin wave? Phys. Lett. A **85**, 375 (1981). doi:10.1016/0375-9601(81)90335-2
91. F.D.M. Haldane, Fractional statistics in arbitrary dimensions: a generalization of the Pauli principle. Phys. Rev. Lett. **67**, 937 (1991). doi:10.1103/PhysRevLett.67.937

92. M.A. Cazalilla, R. Citro, T. Giamarchi, E. Orignac, M. Rigol, One dimensional bosons: from condensed matter systems to ultracold gases. Rev. Mod. Phys. **83**, 1405 (2011). doi:10.1103/RevModPhys.83.1405
93. L. Balents, Spin liquids in frustrated magnets. Nature **464**, 199 (2010). doi:10.1038/nature08917
94. C. Lhuillier, G. Misguich, Introduction to quantum spin liquids, in *Introduction to Frustrated Magnetism*, ed. by C. Lacroix, F. Mila, P. Mendels (Springer, Berlin, 2011), pp. 23–44. doi:10.1007/978-3-642-10589-0
95. L. Savary, L. Balents, Quantum Spin Liquids (2016), arXiv:1601.03742
96. P. Anderson, Resonating valence bonds: a new kind of insulator? Mater. Res. Bull. **8**, 153 (1973). doi:10.1016/0025-5408(73)90167-0
97. P.W. Anderson, The resonating valence bond state in La_2CuO_4 and superconductivity. Science **235**, 1196 (1987). doi:10.1126/science.235.4793.1196
98. S. Yan, D.A. Huse, S.R. White, Spin-liquid ground state of the S = 1/2 Kagome Heisenberg antiferromagnet. Science **332**, 1173 (2011). doi:10.1126/science.1201080
99. H.-C. Jiang, Z. Wang, L. Balents, Identifying topological order by entanglement entropy. Nat. Phys. **8**, 902 (2012). doi:10.1038/nphys2465
100. Y. Iqbal, F. Becca, S. Sorella, D. Poilblanc, Gapless spin-liquid phase in the kagome spin-1/2 Heisenberg antiferromagnet. Phys. Rev. B **87**, 060405 (2013). doi:10.1103/PhysRevB.87.060405
101. Z. Zhu, S.R. White, Spin liquid phase of the S = 1/2 J_1-J_2 Heisenberg model on the triangular lattice. Phys. Rev. B **92**, 041105 (2015). doi:10.1103/PhysRevB.92.041105
102. W.-J. Hu, S.-S. Gong, W. Zhu, D.N. Sheng, Competing spin-liquid states in the spin-1/2 Heisenberg model on the triangular lattice. Phys. Rev. B **92**, 140403 (2015). doi:10.1103/PhysRevB.92.140403
103. X.G. Wen, Topological order in rigid states. Int. J. Mod. Phys. B **04**, 239 (1990). doi:10.1142/S0217979290000139
104. B. Zeng, X. Chen, D.-L. Zhou, X.-G. Wen, Quantum Information Meets Quantum Matter – From Quantum Entanglement to Topological Phase in Many-Body Systems (2015), arXiv:1508.02595
105. X.G. Wen, Vacuum degeneracy of chiral spin states in compactified space. Phys. Rev. B **40**, 7387 (1989). doi:10.1103/PhysRevB.40.7387
106. D.P. Arovas, J.R. Schrieffer, F. Wilczek, Fractional statistics and the quantum hall effect. Phys. Rev. Lett. **53**, 722 (1984). doi:10.1103/PhysRevLett.53.722
107. B.I. Halperin, Statistics of quasiparticles and the hierarchy of fractional quantized Hall states. Phys. Rev. Lett. **52**, 1583 (1984). doi:10.1103/PhysRevLett.52.1583
108. X.G. Wen, Non-Abelian statistics in the fractional quantum Hall states. Phys. Rev. Lett. **66**, 802 (1991). doi:10.1103/PhysRevLett.66.802
109. G. Moore, N. Read, Nonabelions in the fractional quantum Hall effect. Nucl. Phys. B **360**, 362 (1991). doi:10.1016/0550-3213(91)90407-o
110. B.I. Halperin, Quantized Hall conductance, current-carrying edge states, and the existence of extended states in a two-dimensional disordered potential. Phys. Rev. B **25**, 2185 (1982). doi:10.1103/PhysRevB.25.2185
111. A.H. MacDonald, Edge states in the fractional-quantum-Hall-effect regime. Phys. Rev. Lett. **64**, 220 (1990). doi:10.1103/PhysRevLett.64.220
112. X.G. Wen, Gapless boundary excitations in the quantum Hall states and in the chiral spin states. Phys. Rev. B **43**, 11025 (1991). doi:10.1103/PhysRevB.43.11025
113. D.C. Tsui, H.L. Stormer, A.C. Gossard, Two-dimensional magnetotransport in the extreme quantum limit. Phys. Rev. Lett. **48**, 1559 (1982). doi:10.1103/PhysRevLett.48.1559
114. R.B. Laughlin, Anomalous quantum Hall effect: an incompressible quantum fluid with fractionally charged excitations. Phys. Rev. Lett. **50**, 1395 (1983). doi:10.1103/PhysRevLett.50.1395
115. E. Dennis, A. Kitaev, A. Landahl, J. Preskill, Topological quantum memory. J. Math. Phys. **43**, 4452 (2002). doi:10.1063/1.1499754

116. A. Kitaev, Fault-tolerant quantum computation by anyons. Ann. Phys. **303**, 2 (2003). doi:10.1016/S0003-4916(02)00018-0
117. D.R. Hartree, The wave mechanics of an atom with a non-coulomb central field. Part I. Theory and methods. Math. Proc. Camb. Philos. Soc. **24**, 89 (1928). doi:10.1017/S0305004100011919
118. D.R. Hartree, The wave mechanics of an atom with a non-coulomb central field. Part II. Some results and discussion. Math. Proc. Camb. Philos. Soc. **24**, 111 (1928). doi:10.1017/S0305004100011920
119. V. Fock, Näherungsmethode zur Lösung des quantenmechanischen Mehrkörperproblems. Zeitschrift für Physik **61**, 126 (1930). doi:10.1007/BF01340294
120. P. Hohenberg, W. Kohn, Inhomogeneous electron gas. Phys. Rev. **136**, B864 (1964). doi:10.1103/PhysRev.136.B864
121. W. Kohn, L.J. Sham, Self-consistent equations including exchange and correlation effects. Phys. Rev. **140**, A1133 (1965). doi:10.1103/PhysRev.140.A1133
122. R.D. Mattuck, *A Guide to Feynman Diagrams in the Many-Body Problem* (Courier Dover Publications, New York, 1976)
123. N. Laflorencie, D. Poilblanc, Simulations of pure and doped low-dimensional spin-1/2 gapped systems, in *Quantum Magnetism*, ed. by U. Schollwöck, J. Richter, D.J.J. Farnell, R.F. Bishop (Springer, Berlin, 2004), pp. 227–252. doi:10.1007/BFb0119595
124. A.M. Läuchli, Numerical simulations of frustrated systems, in *Introduction to Frustrated Magnetism*, ed. by C. Lacroix, P. Mendels, F. Mila (Springer, Berlin, 2011), pp. 481–511. doi:10.1007/978-3-642-10589-0
125. C. Lanczos, An iteration method for the solution of the eigenvalue problem of linear differential and integral operators. J. Res. Natl. Bur. Stand. **45**, 255 (1950)
126. A.M. Läuchli, An exact diagonalization perspective on the S = 1/2 Kagome Heisenberg antiferromagnet, in *KITP Program: Frustrated Magnetism and Quantum Spin Liquids: From Theory and Models to Experiments*, 13 August–9 November 2012 (2012), http://online.kitp.ucsb.edu/online/fragnets12/laeuchli/
127. N. Metropolis, A.W. Rosenbluth, M.N. Rosenbluth, A.H. Teller, E. Teller, Equation of state calculations by fast computing machines. J. Chem. Phys. **21**, 1087 (1953). doi:10.1063/1.1699114
128. A.W. Sandvik, J. Kurkijärvi, Quantum Monte Carlo simulation method for spin systems. Phys. Rev. B **43**, 5950 (1991). doi:10.1103/PhysRevB.43.5950
129. M. Troyer, U.-J. Wiese, Computational complexity and fundamental limitations to fermionic quantum Monte Carlo simulations. Phys. Rev. Lett. **94**, 170201 (2005). doi:10.1103/PhysRevLett.94.170201
130. M.P. Gelfand, R.R.P. Singh, High-order convergent expansions for quantum many particle systems. Adv. Phys. **49**, 93 (2000). doi:10.1080/000187300243390
131. F. Wegner, Flow-equations for Hamiltonians. Annalen der Physik **506**, 77 (1994). doi:10.1002/andp.19945060203
132. C. Knetter, A. Bühler, E. Müller-Hartmann, G.S. Uhrig, Dispersion and symmetry of bound states in the Shastry–Sutherland model. Phys. Rev. Lett. **85**, 3958 (2000). doi:10.1103/PhysRevLett.85.3958
133. S. Kehrein, *The Flow Equation Approach to Many-Particle Systems* (Springer, Berlin, 2006)
134. J.C. Slater, The theory of complex spectra. Phys. Rev. **34**, 1293 (1929). doi:10.1103/PhysRev.34.1293
135. J.C. Slater, Note on Hartree's method. Phys. Rev. **35**, 210 (1930). doi:10.1103/PhysRev.35.210.2
136. E.P. Gross, Structure of a quantized vortex in boson systems. Il Nuovo Cimento **20**, 454 (1961). doi:10.1007/BF02731494
137. L.P. Pitaevskii, Vortex lines in an imperfect Bose gas. Sov. Phys. JETP **40** (1961)
138. J. Bardeen, L.N. Cooper, J.R. Schrieffer, Microscopic theory of superconductivity. Phys. Rev. **106**, 162 (1957). doi:10.1103/PhysRev.106.162

139. J. Bardeen, L.N. Cooper, J.R. Schrieffer, Theory of superconductivity. Phys. Rev. **108**, 1175 (1957). doi:10.1103/PhysRev.108.1175
140. S. Sorella, Wave function optimization in the variational Monte Carlo method. Phys. Rev. B **71**, 241103 (2005). doi:10.1103/PhysRevB.71.241103
141. F. Becca, L. Capriotti, A. Parola, S. Sorella, Variational wave functions for frustrated magnetic models, in *Introduction to Frustrated Magnetism*, ed. by C. Lacroix, P. Mendels, F. Mila (Springer, Berlin, 2011), pp. 379–406. doi:10.1007/978-3-642-10589-0
142. Y. Iqbal, D. Poilblanc, F. Becca, Spin-1/2 Heisenberg J_1-J_2 antiferromagnet on the kagome lattice. Phys. Rev. B **91**, 020402 (2015). doi:10.1103/PhysRevB.91.020402
143. V.E. Korepin, N.M. Bogoliubov, A.G. Izergin, *Quantum Inverse Scattering Method and Correlation Functions* (Cambridge University Press, Cambridge, 1997)
144. M. Gaudin, *The Bethe Wavefunction* (Cambridge University Press, Cambridge, 2014)
145. B. Sutherland, *Beautiful Models: 70 Years of Exactly Solved Quantum Many-body Problems* (World Scientific, Singapore, 2004)
146. C.N. Yang, C.P. Yang, One-dimensional chain of anisotropic spin-spin interactions. I. Proof of Bethe's hypothesis for ground state in a finite system. Phys. Rev. **150**, 321 (1966). doi:10.1103/PhysRev.150.321
147. C.N. Yang, C.P. Yang, One-dimensional chain of anisotropic spin-spin interactions. II. Properties of the ground-state energy per lattice site for an infinite system. Phys. Rev. **150**, 327 (1966). doi:10.1103/PhysRev.150.327
148. C.N. Yang, C.P. Yang, One-dimensional chain of anisotropic spin-spin interactions III. Applications. Phys. Rev. **151**, 258 (1966). doi:10.1103/PhysRev.151.258
149. R.J. Baxter, One-dimensional anisotropic Heisenberg chain. Ann. Phys. **70**, 323 (1972). doi:10.1016/0003-4916(72)90270-9
150. E.H. Lieb, F. Wu, Absence of Mott transition in an exact solution of the short-range, one-band model in one dimension. Phys. Rev. Lett. **20**, 1445 (1968). doi:10.1103/PhysRevLett.20.1445
151. E.H. Lieb, W. Liniger, Exact analysis of an interacting bose gas. I. The general solution and the ground state. Phys. Rev. **130**, 1605 (1963). doi:10.1103/PhysRev.130.1605
152. E.H. Lieb, Exact analysis of an interacting bose gas II. The excitation spectrum. Phys. Rev. **130**, 1616 (1963). doi:10.1103/PhysRev.130.1616
153. C.N. Yang, C.P. Yang, Thermodynamics of a one-dimensional system of Bosons with repulsive delta-function interaction. J. Math. Phys. **10**, 1115 (1969). doi:10.1063/1.1664947
154. M. Takahashi, *Thermodynamics of One-Dimensional Solvable Models* (Cambridge University Press, Cambridge, 2005)
155. F.H.L. Essler, R.M. Konik, Application of massive integrable quantum field theories to problems in condensed matter physics, *From Fields to Strings: Circumnavigating Theoretical Physics* (World Scientific, Singapore, 2005), pp. 684–830. doi:10.1142/9789812775344_0020
156. A.B. Zamolodchikov, Exact two-particle S-matrix of quantum sine-Gordon solitons. Commun. Math. Phys. **55**, 183 (1977). doi:10.1007/BF01626520
157. G. Mussardo, *Statistical Field Theory: An Introduction to Exactly Solved Models in Statistical Physics* (Oxford University Press, Oxford, 2009)
158. C.N. Yang, Some exact results for the many-body problem in one dimension with repulsive delta-function interaction. Phys. Rev. Lett. **19**, 1312 (1967). doi:10.1103/PhysRevLett.19.1312
159. N.A. Slavnov, Calculation of scalar products of wave functions and form factors in the framework of the algebraic Bethe ansatz. Theor. Math. Phys. **79**, 502 (1989). doi:10.1007/BF01016531
160. N.A. Slavnov, Nonequal-time current correlation function in a one-dimensional Bose gas. Theor. Math. Phys. **82**, 273 (1990). doi:10.1007/BF01029221
161. N. Kitanine, J. Maillet, V. Terras, Form factors of the XXZ Heisenberg finite chain. Nucl. Phys. B **554**, 647 (1999). doi:10.1016/S0550-3213(99)00295-3
162. N. Kitanine, J. Maillet, V. Terras, Correlation functions of the XXZ Heisenberg spin chain in a magnetic field. Nucl. Phys. B **567**, 554 (2000). doi:10.1016/S0550-3213(99)00619-7

163. R.M. Konik, Haldane-gapped spin chains: exact low-temperature expansions of correlation functions. Phys. Rev. B **68**, 104435 (2003). doi:10.1103/PhysRevB.68.104435
164. F.H.L. Essler, R.M. Konik, Finite-temperature lineshapes in gapped quantum spin chains. Phys. Rev. B **78**, 100403 (2008). doi:10.1103/PhysRevB.78.100403
165. A. James, F.H.L. Essler, R.M. Konik, Finite-temperature dynamical structure factor of alternating Heisenberg chains. Phys. Rev. B **78**, 094411 (2008). doi:10.1103/PhysRevB.78.094411
166. F.H.L. Essler, R.M. Konik, Finite-temperature dynamical correlations in massive integrable quantum field theories. J. Stat. Mech. Theory Exp. **2009**, P09018 (2009). doi:10.1088/1742-5468/2009/09/P09018
167. W.D. Goetze, U. Karahasanovic, F.H.L. Essler, Low-temperature dynamical structure factor of the two-leg spin-1/2 Heisenberg ladder. Phys. Rev. B **82**, 104417 (2010). doi:10.1103/PhysRevB.82.104417
168. D.A. Tennant, B. Lake, A.J.A. James, F.H.L. Essler, S. Notbohm, H.-J. Mikeska, J. Fielden, P. Kögerler, P.C. Canfield, M.T.F. Telling, Anomalous dynamical line shapes in a quantum magnet at finite temperature. Phys. Rev. B **85**, 014402 (2012). doi:10.1103/PhysRevB.85.014402
169. M. Rigol, V. Dunjko, V. Yurovsky, M. Olshanii, Relaxation in a completely integrable many-body quantum system: an ab initio study of the dynamics of the highly excited states of 1D lattice hard-core Bosons. Phys. Rev. Lett. **98**, 4 (2007). doi:10.1103/PhysRevLett.98.050405
170. M. Fagotti, F.H.L. Essler, Stationary behaviour of observables after a quantum quench in the spin-1/2 Heisenberg XXZ chain. J. Stat. Mech. Theory Exp. **2013**, P07012 (2013). doi:10.1088/1742-5468/2013/07/P07012
171. M. Fagotti, M. Collura, F.H.L. Essler, P. Calabrese, Relaxation after quantum quenches in the spin-1/2 Heisenberg XXZ chain. Phys. Rev. B **89**, 125101 (2014). doi:10.1103/PhysRevB.89.125101
172. E. Ilievski, M. Medenjak, T. Prosen, Quasilocal conserved operators in isotropic Heisenberg spin 1/2 chain (2015), arXiv:1506.05049
173. E. Ilievski, J. De Nardis, B. Wouters, J.-S. Caux, F.H.L. Essler, T. Prosen, Complete generalized Gibbs ensembles in an interacting theory. Phys. Rev. Lett. **115**, 157201 (2015). doi:10.1103/PhysRevLett.115.157201
174. E.T. Jaynes, Information theory and statistical mechanics. Phys. Rev. **106**, 171 (1957). doi:10.1103/PhysRev.106.620
175. E.T. Jaynes, Information theory and statistical mechanics II. Phys. Rev. **108**, 171 (1957). doi:10.1103/PhysRev.108.171
176. D. Fioretto, G. Mussardo, Quantum quenches in integrable field theories. New J. Phys. **12**, 055015 (2010). doi:10.1088/1367-2630/12/5/055015
177. M. Fagotti, F.H.L. Essler, Reduced density matrix after a quantum quench. Phys. Rev. B **87**, 245107 (2013). doi:10.1103/PhysRevB.87.245107
178. F.H.L. Essler, G. Mussardo, M. Panfil, Generalized Gibbs ensembles for quantum field theories. Phys. Rev. A **91**, 051602 (2015). doi:10.1103/PhysRevA.91.051602
179. F.H.L. Essler, S. Kehrein, S.R. Manmana, N.J. Robinson, Quench dynamics in a model with tuneable integrability breaking. Phys. Rev. B **89**, 165104 (2014). doi:10.1103/PhysRevB.89.165104
180. S. Sotiriadis, Zamolodchikov–Faddeev algebra and quantum quenches in integrable field theories. J. Stat. Mech. Theory Exp. **2012**, P02017 (2012), http://iopscience.iop.org/1742-5468/2012/02/P02017
181. J.-S. Caux, R.M. Konik, Constructing the generalized Gibbs ensemble after a quantum quench. Phys. Rev. Lett. **109**, 175301 (2012). doi:10.1103/PhysRevLett.109.175301
182. J. Mossel, J.-S. Caux, Generalized TBA and generalized Gibbs. J. Phys. A Math. Theor. **45**, 255001 (2012). doi:10.1088/1751-8113/45/25/255001
183. E. Demler, A.M. Tsvelik, Universal features of the excitation spectrum in a generalized Gibbs distribution ensemble. Phys. Rev. B **86**, 115448 (2012). doi:10.1103/PhysRevB.86.115448
184. L. Bonnes, F.H.L. Essler, A.M. Läuchli, Light-cone dynamics after quantum quenches in spin chains. Phys. Rev. Lett. **113**, 187203 (2014). doi:10.1103/PhysRevLett.113.187203

185. M. Kollar, F.A. Wolf, M. Eckstein, Generalized Gibbs ensemble prediction of prethermalization plateaus and their relation to nonthermal steady states in integrable systems. Phys. Rev. B **84**, 054304 (2011). doi:10.1103/PhysRevB.84.054304
186. M. Fagotti, On conservation laws, relaxation and pre-relaxation after a quantum quench. J. Stat. Mech. Theory Exp. **2014**, P03016 (2014). doi:10.1088/1742-5468/2014/03/P03016
187. B. Bertini, F.H.L. Essler, S. Groha, N.J. Robinson, Prethermalization and thermalization in models with weak integrability breaking. Phys. Rev. Lett. **115**, 180601 (2015). doi:10.1103/PhysRevLett.115.180601
188. T. Langen, T. Gasenzer, J. Schmiedmayer, Prethermalization and universal dynamics in near-integrable quantum systems. J. Stat. Mech. Theory Exp. **2016**, 064009 (2016), http://stacks.iop.org/1742-5468/2016/i=6/a=064009
189. F. Verstraete, V. Murg, J.I. Cirac, Matrix product states, projected entangled pair states, and variational renormalization group methods for quantum spin systems. Adv. Phys. **57**, 143 (2008). doi:10.1080/14789940801912366
190. N. Schuch, Condensed Matter Applications of Entanglement Theory (2013), arXiv:1306.5551
191. R. Orús, A practical introduction to tensor networks: matrix product states and projected entangled pair states. Ann. Phys. **349**, 117 (2014). doi:10.1016/j.aop.2014.06.013
192. K.G. Wilson, The renormalization group: critical phenomena and the Kondo problem. Rev. Mod. Phys. **47**, 773 (1975). doi:10.1103/RevModPhys.47.773
193. J. Kondo, Resistance minimum in dilute magnetic alloys. Prog. Theor. Phys. **32**, 37 (1964). doi:10.1143/PTP.32.37
194. P.W. Anderson, Localized magnetic states in metals. Phys. Rev. **124**, 41 (1961). doi:10.1103/PhysRev.124.41
195. A.C. Hewson, *The Kondo Problem to Heavy Fermions* (Cambridge University Press, Cambridge, 1993)
196. R. Bulla, T. Costi, T. Pruschke, Numerical renormalization group method for quantum impurity systems. Rev. Mod. Phys. **80**, 395 (2008). doi:10.1103/RevModPhys.80.395
197. S.R. White, R.M. Noack, Real-space quantum renormalization groups. Phys. Rev. Lett. **68**, 3487 (1992). doi:10.1103/PhysRevLett.68.3487
198. S.R. White, Density matrix formulation for quantum renormalization groups. Phys. Rev. Lett. **69**, 2863 (1992). doi:10.1103/PhysRevLett.69.2863
199. S.R. White, Density-matrix algorithms for quantum renormalization groups. Phys. Rev. B **48**, 10345 (1993). doi:10.1103/PhysRevB.48.10345
200. J.I. Latorre, E. Rico, G. Vidal, Ground state entanglement in quantum spin chains. Quantum Inf. Comput. **4**, 48 (2004), arXiv:0304098
201. U. Schollwöck, The density-matrix renormalization group. Rev. Mod. Phys. **77**, 259 (2005). doi:10.1103/RevModPhys.77.259
202. U. Schollwöck, The density-matrix renormalization group in the age of matrix product states. Ann. Phys. **326**, 96 (2011). doi:10.1016/j.aop.2010.09.012
203. S.R. White, D. Huse, Numerical renormalization-group study of low-lying eigenstates of the antiferromagnetic S = 1 Heisenberg chain. Phys. Rev. B **48**, 3844 (1993). doi:10.1103/PhysRevB.48.3844
204. I. Peschel, X. Wang, M. Kaulke, K. Hallberg, Density-Matrix Renormalization - A New Numerical Method in Physics (Springer, Berlin, 1999). doi:10.1007/BFb0106062
205. K. Hallberg, Density Matrix Renormalization: A Review of the Method and its Applications (2003), arXiv:0303557
206. S. Östlund, S. Rommer, Thermodynamic limit of the density matrix renormalization for the spin-1 Heisenberg chain. Phys. Rev. Lett. **75**, 13 (1995). doi:10.1103/PhysRevLett.75.3537
207. S. Rommer, S. Östlund, Class of ansatz wave functions for one-dimensional spin systems and their relation to the density matrix renormalization group. Phys. Rev. B **55**, 2164 (1997). doi:10.1103/PhysRevB.55.2164
208. J. Dukelsky, M.A. Martín-Delgado, T. Nishino, G. Sierra, Equivalence of the variational matrix product method and the density matrix renormalization group applied to spin chains. Europhys. Lett. **43**, 457 (1998). doi:10.1209/epl/i1998-00381-x

209. I.P. McCulloch, From density-matrix renormalization group to matrix product states. J. Stat. Mech. Theory Exp. **2007**, P10014 (2007). doi:10.1088/1742-5468/2007/10/P10014
210. C.K. Majumdar, D.K. Ghosh, On next-nearest-neighbor interaction in linear chain I. J. Math. Phys. **10**, 1388 (1969). doi:10.1063/1.1664978
211. C.K. Majumdar, D.K. Ghosh, On Next-Nearest-Neighbor Interaction in Linear Chain II. J. Math. Phys. **10**, 1388 (1969). doi:10.1063/1.1664978
212. C.K. Majumdar, Antiferromagnetic model with known ground state. J. Phys. C Solid State Phys. **3**, 911 (1970). doi:10.1088/0022-3719/3/4/019
213. M. Fannes, B. Nachtergaele, R.F. Werner, Finitely correlated states on quantum spin chains. Commun. Math. Phys. **144**, 443 (1992). doi:10.1007/BF02099178
214. G. Vidal, Efficient classical simulation of slightly entangled quantum computations. Phys. Rev. Lett. **91**, 4 (2003). doi:10.1103/PhysRevLett.91.147902
215. G. Vidal, Efficient simulation of one-dimensional quantum many-body systems. Phys. Rev. Lett. **93**, 4 (2004). doi:10.1103/PhysRevLett.93.040502
216. F. Verstraete, J.I. Cirac, Valence-bond states for quantum computation. Phys. Rev. A **70**, 060302 (2004). doi:10.1103/PhysRevA.70.060302
217. F. Verstraete, D. Porras, J.I. Cirac, Density matrix renormalization group and periodic boundary conditions: a quantum information perspective. Phys. Rev. Lett. **93**, 227205 (2004). doi:10.1103/PhysRevLett.93.227205
218. C. Schön, E. Solano, F. Verstraete, J.I. Cirac, M.M. Wolf, Sequential generation of entangled multiqubit states. Phys. Rev. Lett. **95**, 4 (2005). doi:10.1103/PhysRevLett.95.110503
219. C. Schön, K. Hammerer, M.M. Wolf, J.I. Cirac, E. Solano, Sequential generation of matrix-product states in cavity QED. Phys. Rev. A **75**, 11 (2007). doi:10.1103/PhysRevA.75.032311
220. T.J. Osborne, J. Eisert, F. Verstraete, Holographic quantum states. Phys. Rev. Lett. **105**, 6 (2010). doi:10.1103/PhysRevLett.105.260401
221. D. Pérez-García, F. Verstraete, M.M. Wolf, J.I. Cirac, Matrix product state representations. Quantum Inf. Comput. **7**, 401 (2007), arXiv:0608197
222. D.E. Evans, R. Hoegh-Krohn, Spectral properties of positive maps on C*-algebras. J. Lond. Math. Soc. **s2-17**, 345 (1978). doi:10.1112/jlms/s2-17.2.345
223. J.I. Cirac, D. Perez-Garcia, N. Schuch, F. Verstraete, Matrix Product Density Operators: Renormalization Fixed Points and Boundary Theories (2016), arXiv:1606.00608
224. N. Schuch, M.M. Wolf, F. Verstraete, J.I. Cirac, Entropy scaling and simulability by matrix product states. Phys. Rev. Lett. **100**, 4 (2008). doi:10.1103/PhysRevLett.100.030504
225. F. Pollmann, S. Mukerjee, A.M. Turner, J.E. Moore, Theory of finite-entanglement scaling at one-dimensional quantum critical points. Phys. Rev. Lett. **102**, 255701 (2009). doi:10.1103/PhysRevLett.102.255701
226. D. Pérez-García, M. Wolf, M. Sanz, F. Verstraete, J.I. Cirac, String order and symmetries in quantum spin lattices. Phys. Rev. Lett. **100**, 167202 (2008). doi:10.1103/PhysRevLett.100.167202
227. N. Schuch, D. Pérez-García, I. Cirac, Classifying quantum phases using matrix product states and projected entangled pair states. Phys. Rev. B **84**, 165139 (2011). doi:10.1103/PhysRevB.84.165139
228. X. Chen, Z.-C. Gu, X.-G. Wen, Classification of gapped symmetric phases in one-dimensional spin systems. Phys. Rev. B **83**, 035107 (2011). doi:10.1103/PhysRevB.83.035107
229. F. Pollmann, E. Berg, A.M. Turner, M. Oshikawa, Symmetry protection of topological phases in one-dimensional quantum spin systems. Phys. Rev. B **85**, 075125 (2012). doi:10.1103/PhysRevB.85.075125
230. G. Vidal, Classical simulation of infinite-size quantum lattice systems in one spatial dimension. Phys. Rev. Lett. **98**, 5 (2007). doi:10.1103/PhysRevLett.98.070201
231. R. Orús, G. Vidal, Infinite time-evolving block decimation algorithm beyond unitary evolution. Phys. Rev. B **78**, 155117 (2008). doi:10.1103/PhysRevB.78.155117
232. J. Haegeman, J.I. Cirac, T.J. Osborne, I. Pizorn, H. Verschelde, F. Verstraete, Time-dependent variational principle for quantum lattices. Phys. Rev. Lett. **107**, 070601 (2011). doi:10.1103/PhysRevLett.107.070601

233. S.R. White, Density matrix renormalization group algorithms with a single center site. Phys. Rev. B **72**, 180403 (2005). doi:10.1103/PhysRevB.72.180403
234. I.P. McCulloch, Infinite size density matrix renormalization group, revisited (2008), arXiv:0804.2509
235. J.A. Kjäll, M.P. Zaletel, R.S.K. Mong, J.H. Bardarson, F. Pollmann, Phase diagram of the anisotropic spin-2 XXZ model: infinite-system density matrix renormalization group study. Phys. Rev. B **87**, 235106 (2013). doi:10.1103/PhysRevB.87.235106
236. J. Haegeman, T.J. Osborne, F. Verstraete, Post-matrix product state methods: to tangent space and beyond. Phys. Rev. B **88**, 075133 (2013). doi:10.1103/PhysRevB.88.075133
237. A. Milsted, J. Haegeman, T.J. Osborne, Matrix product states and variational methods applied to critical quantum field theory. Phys. Rev. D **88**, 085030 (2013). doi:10.1103/PhysRevD.88.085030
238. J. Haegeman, M. Mariën, T.J. Osborne, F. Verstraete, Geometry of matrix product states: metric, parallel transport, and curvature. J. Math. Phys. **55**, 021902 (2014). doi:10.1063/1.4862851
239. P. Pippan, S.R. White, H.G. Evertz, Efficient matrix-product state method for periodic boundary conditions. Phys. Rev. B **81**, 81103 (2010). doi:10.1103/PhysRevB.81.081103
240. B. Pirvu, F. Verstraete, G. Vidal, Exploiting translational invariance in matrix product state simulations of spin chains with periodic boundary conditions. Phys. Rev. B **83**, 125104 (2011). doi:10.1103/PhysRevB.83.125104
241. D. Porras, F. Verstraete, J.I. Cirac, Renormalization algorithm for the calculation of spectra of interacting quantum systems. Phys. Rev. B **73** (2006). doi:10.1103/PhysRevB.73.014410
242. B. Pirvu, V. Murg, J.I. Cirac, F. Verstraete, Matrix product operator representations. New J. Phys. **12**, 025012 (2010). doi:10.1088/1367-2630/12/2/025012
243. A.J. Daley, C. Kollath, U. Schollwöck, G. Vidal, Time-dependent density-matrix renormalization-group using adaptive effective Hilbert spaces. J. Stat. Mech. Theory Exp. **2004**, P04005 (2004). doi:10.1088/1742-5468/2004/04/P04005
244. S.R. White, A.E. Feiguin, Real-time evolution using the density matrix renormalization group. Phys. Rev. Lett. **93**, 076401 (2004). doi:10.1103/PhysRevLett.93.076401
245. F. Verstraete, J.J. García-Ripoll, J.I. Cirac, Matrix product density operators: simulation of finite-temperature and dissipative systems. Phys. Rev. Lett. **93**, 207204 (2004). doi:10.1103/PhysRevLett.93.207204
246. J. Haegeman, C. Lubich, I. Oseledets, B. Vandereycken, F. Verstraete, Unifying time evolution and optimization with matrix product states (2014), arXiv:1408.5056
247. V. Zauner, M. Ganahl, H.G. Evertz, T. Nishino, Time evolution within a comoving window: scaling of signal fronts and magnetization plateaus after a local quench in quantum spin chains. J. Phys. Condens. Matter **27**, 425602 (2012). doi:10.1088/0953-8984/27/42/425602
248. H.N. Phien, G. Vidal, I.P. McCulloch, Infinite boundary conditions for matrix product state calculations. Phys. Rev. B **86**, 245107 (2012). doi:10.1103/PhysRevB.86.245107
249. A. Milsted, J. Haegeman, T.J. Osborne, F. Verstraete, Variational matrix product ansatz for nonuniform dynamics in the thermodynamic limit. Phys. Rev. B **88**, 155116 (2013). doi:10.1103/PhysRevB.88.155116
250. K. Hallberg, Density-matrix algorithm for the calculation of dynamical properties of low-dimensional systems. Phys. Rev. B **52**, R9827 (1995). doi:10.1103/PhysRevB.52.R9827
251. P.E. Dargel, A. Honecker, R. Peters, R.M. Noack, T. Pruschke, Adaptive Lanczos-vector method for dynamic properties within the density matrix renormalization group. Phys. Rev. B **83**, 161104 (2011). doi:10.1103/PhysRevB.83.161104
252. P.E. Dargel, A. Wöllert, A. Honecker, I.P. McCulloch, U. Schollwöck, T. Pruschke, Lanczos algorithm with matrix product states for dynamical correlation functions. Phys. Rev. B **85**, 205119 (2012). doi:10.1103/PhysRevB.85.205119
253. S. Ramasesha, S.K. Pati, H.R. Krishnamurthy, Z. Shuai, J.L. Brédas, Symmetrized density-matrix renormalization-group method for excited states of Hubbard models. Phys. Rev. B **54**, 7598 (1996). doi:10.1103/PhysRevB.54.7598

254. T. Kühner, S. White, Dynamical correlation functions using the density matrix renormalization group. Phys. Rev. B **60**, 335 (1999). doi:10.1103/PhysRevB.60.335
255. E. Jeckelmann, Dynamical density-matrix renormalization-group method. Phys. Rev. B **66**, 045114 (2002). doi:10.1103/PhysRevB.66.045114
256. A. Weichselbaum, F. Verstraete, U. Schollwöck, J.I. Cirac, J. von Delft, Variational matrix-product-state approach to quantum impurity models. Phys. Rev. B **80**, 165117 (2009). doi:10.1103/PhysRevB.80.165117
257. S.R. White, I. Affleck, Spectral function for the S = 1 Heisenberg antiferromagetic chain. Phys. Rev. B **77**, 134437 (2008). doi:10.1103/PhysRevB.77.134437
258. R. Pereira, S. White, I. Affleck, Exact edge singularities and dynamical correlations in spin-1/2 chains. Phys. Rev. Lett. **100**, 4 (2008). doi:10.1103/PhysRevLett.100.027206
259. T. Barthel, U. Schollwöck, S. White, Spectral functions in one-dimensional quantum systems at finite temperature using the density matrix renormalization group. Phys. Rev. B **79**, 245101 (2009). doi:10.1103/PhysRevB.79.245101
260. J. Kjäll, F. Pollmann, J. Moore, Bound states and E_{8} symmetry effects in perturbed quantum Ising chains. Phys. Rev. B **83**, 020407 (2011). doi:10.1103/PhysRevB.83.020407
261. L. Seabra, F. Pollmann, Exotic Ising dynamics in a Bose-Hubbard model. Phys. Rev. B **88**, 5 (2013). doi:10.1103/PhysRevB.88.125103
262. A. Holzner, A. Weichselbaum, I.P. McCulloch, U. Schollwöck, J. von Delft, Chebyshev matrix product state approach for spectral functions. Phys. Rev. B **83**, 195115 (2011). doi:10.1103/PhysRevB.83.195115
263. A. Feiguin, S. White, Finite-temperature density matrix renormalization using an enlarged Hilbert space. Phys. Rev. B **72**, 220401 (2005). doi:10.1103/PhysRevB.72.220401
264. S. White, Minimally entangled typical quantum states at finite temperature. Phys. Rev. Lett. **102**, 190601 (2009). doi:10.1103/PhysRevLett.102.190601
265. C. Karrasch, J.H. Bardarson, J.E. Moore, Finite-temperature dynamical density matrix renormalization group and the drude weight of spin-1/2 chains. Phys. Rev. Lett. **108**, 227206 (2012). doi:10.1103/PhysRevLett.108.227206
266. S.R. White, Spin gaps in a frustrated Heisenberg model for CaV_4O_9. Phys. Rev. Lett. **77**, 3633 (1996). doi:10.1103/PhysRevLett.77.3633
267. E. Stoudenmire, S.R. White, Studying two-dimensional systems with the density matrix renormalization group. Annu. Rev. Condens. Matter Phys. **3**, 111 (2012). doi:10.1146/annurev-conmatphys-020911-125018
268. F. Verstraete, J.I. Cirac, Renormalization algorithms for Quantum-Many Body Systems in two and higher dimensions (2004), arXiv:0407066
269. D. Perez-Garcia, F. Verstraete, J.I. Cirac, M.M. Wolf, PEPS as unique ground states of local Hamiltonians. Quantum Inf. Comput. **8**, 0650 (2007), http://www.rintonpress.com/journals/qiconline.html
270. F. Verstraete, M.M. Wolf, D. Perez-Garcia, J.I. Cirac, Criticality, the area law, and the computational power of projected entangled pair states. Phys. Rev. Lett. **96**, 220601 (2006). doi:10.1103/PhysRevLett.96.220601
271. N. Schuch, D. Poilblanc, J.I. Cirac, D. Pérez-García, Resonating valence bond states in the PEPS formalism. Phys. Rev. B **86**, 115108 (2012). doi:10.1103/PhysRevB.86.115108
272. Z.-C. Gu, M. Levin, B. Swingle, X.-G. Wen, Tensor-product representations for string-net condensed states. Phys. Rev. B **79**, 085118 (2009). doi:10.1103/PhysRevB.79.085118
273. O. Buerschaper, M. Aguado, G. Vidal, Explicit tensor network representation for the ground states of string-net models. Phys. Rev. B **79**, 085119 (2009). doi:10.1103/PhysRevB.79.085119
274. N. Schuch, M. Wolf, F. Verstraete, J.I. Cirac, Computational complexity of projected entangled pair states. Phys. Rev. Lett. **98**, 140506 (2007). doi:10.1103/PhysRevLett.98.140506
275. J.I. Cirac, D. Poilblanc, N. Schuch, F. Verstraete, Entanglement spectrum and boundary theories with projected entangled-pair states. Phys. Rev. B **83**, 245134 (2011). doi:10.1103/PhysRevB.83.245134

276. N. Schuch, D. Poilblanc, J.I. Cirac, D. Pérez-García, Topological order in the projected entangled-pair states formalism: transfer operator and boundary Hamiltonians. Phys. Rev. Lett. **111**, 090501 (2013). doi:10.1103/PhysRevLett.111.090501
277. S. Yang, L. Lehman, D. Poilblanc, K. Van Acoleyen, F. Verstraete, J.I. Cirac, N. Schuch, Edge theories in projected entangled pair state models. Phys. Rev. Lett. **112**, 036402 (2014). doi:10.1103/PhysRevLett.112.036402
278. N. Schuch, J.I. Cirac, D. Pérez-García, PEPS as ground states: degeneracy and topology. Ann. Phys. **325**, 2153 (2010). doi:10.1016/j.aop.2010.05.008
279. O. Buerschaper, Twisted injectivity in projected entangled pair states and the classification of quantum phases. Ann. Phys. **351**, 447 (2014). doi:10.1016/j.aop.2014.09.007
280. M.B. Şahinoğlu, D. Williamson, N. Bultinck, M. Mariën, J. Haegeman, N. Schuch, F. Verstraete, Characterizing Topological Order with Matrix Product Operators (2014), arXiv:1409.2150
281. N. Bultinck, M. Mariën, D.J. Williamson, M.B. Şahinoğlu, J. Haegeman, F. Verstraete, Anyons and matrix product operator algebras (2015), arXiv:1511.08090
282. J. Haegeman, V. Zauner, N. Schuch, F. Verstraete, Shadows of anyons and the entanglement structure of topological phases. Nat. Commun. **6**, 8284 (2015). doi:10.1038/ncomms9284
283. M. Mariën, J. Haegeman, P. Fendley, F. Verstraete, Condensation-Driven Phase Transitions in Perturbed String Nets (2016), arXiv:1607.05296
284. G. Vidal, Entanglement renormalization. Phys. Rev. Lett. **99**, 220405 (2007). doi:10.1103/PhysRevLett.99.220405
285. F. Verstraete, J.I. Cirac, J. Latorre, E. Rico, M. Wolf, Renormalization-group transformations on quantum states. Phys. Rev. Lett. **94**, 5 (2005). doi:10.1103/PhysRevLett.94.140601
286. G. Evenbly, G. Vidal, Algorithms for entanglement renormalization: boundaries, impurities and interfaces. J. Stat. Phys. **157**, 931 (2014). doi:10.1007/s10955-014-0983-1
287. V. Zauner, D. Draxler, L. Vanderstraeten, M. Degroote, J. Haegeman, M.M. Rams, V. Stojevic, N. Schuch, F. Verstraete, Transfer matrices and excitations with matrix product states. New J. Phys. **17**, 053002 (2015). doi:10.1088/1367-2630/17/5/053002
288. M. Bal, M.M. Rams, V. Zauner, J. Haegeman, F. Verstraete, Matrix product state renormalization (2015), arXiv:1509.01522
289. F. Verstraete, J.I. Cirac, Continuous matrix product states for quantum fields. Phys. Rev. Lett. **104** (2010). doi:10.1103/PhysRevLett.104.190405
290. J. Haegeman, J.I. Cirac, T.J. Osborne, H. Verschelde, F. Verstraete, Applying the variational principle to $(1 + 1)$-dimensional quantum field theories. Phys. Rev. Lett. **105**, 251601 (2010). doi:10.1103/PhysRevLett.105.251601
291. J. Haegeman, J.I. Cirac, T.J. Osborne, F. Verstraete, Calculus of continuous matrix product states. Phys. Rev. B **88**, 085118 (2013). doi:10.1103/PhysRevB.88.085118
292. D. Draxler, J. Haegeman, T.J. Osborne, V. Stojevic, L. Vanderstraeten, F. Verstraete, Particles, holes, and solitons: a matrix product state approach. Phys. Rev. Lett. **111**, 020402 (2013). doi:10.1103/PhysRevLett.111.020402
293. J. Rincon, M. Ganahl, G. Vidal, Lieb-Liniger model with exponentially-decaying interactions: a continuous matrix product state study. Phys. Rev. B **92**, 115107 (2015). doi:10.1103/PhysRevB.92.115107
294. D. Draxler, J. Haegeman, F. Verstraete, M. Rizzi, Atomtronics - a continuous matrix product state approach (2016), arXiv:1609.09704
295. J. Haegeman, D. Draxler, V. Stojevic, J.I. Cirac, T.J. Osborne, F. Verstraete, Quantum Gross–Pitaevskii Equation (2015), arXiv:1501.06575
296. K. Wilson, J.B. Kogut, The renormalization group and the ϵ expansion. Phys. Rep. **12**, 75 (1974). doi:10.1016/0370-1573(74)90023-4
297. M.E. Peskin, D.V. Schroeder, *An Introduction to Quantum Field Theory* (Westview Press, Colorado, 1995)
298. E. Fradkin, *Field Theories of Condensed Matter Physics*, 2nd edn. (Cambridge University Press, Cambridge, 2013)
299. P. Nozières, *Theory Of Interacting Fermi Systems* (W.A. Benjamin Inc., 1964)

300. R. Shankar, Renormalization-group approach to interacting fermions. Rev. Mod. Phys. **66**, 129 (1994). doi:10.1103/RevModPhys.66.129
301. L.D. Landau, Oscillations in a Fermi liquid. JETP **30**, 1058 (1956)
302. L.D. Landau, The theory of a Fermi liquid. JETP **3**, 920 (1957)

http://www.springer.com/978-3-319-64190-4

Tensor Network States and Effective Particles for
Low-Dimensional Quantum Spin Systems
Vanderstraeten, L.
2017, XIII, 219 p. 54 illus., 48 illus. in color., Hardcover
ISBN: 978-3-319-64190-4